



© 2018 CERN

[Introduction](#) • [Information for users coming to ISOLDE in 2018](#)

#### **ISOLDE facility**

[Target and Ion Source Development](#) • [RILIS Report for 2017](#) • [Summary of the Operations of REX/HIE-ISOLDE during the 2017 Campaign](#)

#### **Ground-state properties**

[High-resolution laser spectroscopy of the neutron-rich tin isotopes](#) • [2017 at the Collinear Resonance Ionization Spectroscopy \(CRIS\) experiment](#) • [Collinear laser spectroscopy of nickel](#) • [Precision mass measurements of n-rich cadmium isotopes with ISOLTRAP](#) • [ISOLTRAP probes the  \$N = 28\$  shell gap and deformation near  \$A = 100\$](#)  • [New territory for IDS – hyperfine structure and isotope shift measurements](#)

#### **Beta-decay studies**

[Beta decay of  \$^{64}\text{Ge}\$  for accurate weak-decay rates](#) • [Electron capture of  \$^8\text{B}\$  into highly excited states of  \$^8\text{Be}\$](#)  • [First  \$\beta\$ -NMR experiments with liquids at VITO](#)

#### **RIB applications to solid-state physics**

[Atomic-scale study of the amorphous-to-crystalline phase transition mechanism in GeTe thin films](#) • [Potassium self-diffusion in single-crystal alkali feldspar](#) • [Copper diffusion in equiatomic CoCrFeNi high-entropy alloy single crystals](#) • [Influence of Fermi-level on the lattice location of  \$^{27}\text{Mg}\$  in GaN](#) • [Results of experiment IS647 in Naturally Layered Perovskites](#) • [Renovation of the emission Mössbauer spectroscopy setup](#)

#### **Studies with post-accelerated beams**

[Towards Identification of Mixed-Symmetry States in  \$N=80\$  Isotones above  \$Z=58\$](#)  • [Coulomb Excitation of Semi-Magic  \$^{206}\text{Hg}\$](#)  • [The  \$^{59}\text{Cu}\(p, \alpha\)\$  cross section and its implications for nucleosynthesis in core collapse supernovae](#) • [Magnetic moments of short-lived excited states](#) • [ISOLDE Solenoidal Spectrometer Progress Update](#) • [A new plunger device for MINIBALL at HIE-ISOLDE](#)

#### **ISOLDE Support**

[Support and Contacts](#)

[isolde.web.cern.ch](http://isolde.web.cern.ch)



## Introduction

*Gerda Neyens: ISOLDE physics group leader*

On July 1, 2017, I took over from Maria Borge as group leader. Maria has made a tremendous and very successful effort during her 5 years of leadership to increase the visibility of ISOLDE at CERN. In December 2014, it was 50 years ago that the CERN management approved the construction of ISOLDE, a fact that was celebrated in the presence of the CERN directors. This coincided nicely with the 60th birthday of CERN itself, founded in 1954. Last year, we celebrated 50 years of physics with radioactive beams at ISOLDE, which started only 2 years after the construction of the building started in 1955! For this occasion, Maria — together with Klaus Blaum — edited a Focus Issue in Journal of Physics G: Nuclear and Particle Physics, including reviews and topical papers on experiments and developments at ISOLDE during the past decade(s). Thanks to financial contributions from CERN, from the ISOLDE collaboration and from MPIK Heidelberg, all papers are now available in 'open access' in this "Focus on Exotic Beams at ISOLDE: A Laboratory Portrait". The papers can be viewed and downloaded at the following link: <http://cern.ch/go/F6nW>.

Hard copies of the volume have been distributed to the lead authors of the 28 contributions in this volume, as well as to the representatives in the ISCC for further distribution in their country.

Exactly 50 years after the first radioactive beam was produced at ISOLDE-I, the CERN communications team with the help of a few local ISOLDE team members, launched a media campaign to celebrate this event and share it with the world. I would like to thank Erwin, Harriet and Christoph for their enormous enthusiasm for organizing this media event and the many hours they spent for its preparation. It all started with a Facebook-live on October 16, 2017. The event itself, as well as the on-line launch of five 10-min videos and short articles about the history and science at ISOLDE was communicated to the world via all possible so-

cial media (Facebook, Twitter, Instagram, YouTube). In the period from mid October till mid November #MeetISOLDE was mentioned 51.700 times! In the week that the ISOLDE videos and articles series were launched, the CERN visibility on social media increased by 15%.

In case you missed the articles series and videos, you can still watch them via a link on ISOLDE's main page <https://isolde.web.cern.ch/isolde-videos>. I recommend that you use them for your outreach activities about ISOLDE and CERN.

During Maria's time as a group leader, the old ISOLDE users building 507 was taken down and a new building 508 was constructed, including user laboratories (lasers, detectors, experimental off-line set-ups, etc..) as well as a control room for the operation of ISOLDE, a kitchen, users offices and most importantly the meeting room with view onto the hall. This has allowed organizing more and more visits to the ISOLDE facility, for VIPs, for schools and students, but also for the broader public. The number of visitors to ISOLDE has increased from 745 in 2014 to 1546 in 2017! The continuously increasing number of visitors has required that one of our fellows coordinates all of these visits and that we initiated a visitors guides training a link to the training presentation is here <http://cern.ch/go/xV9B> for our in-house group to be well prepared to help with the visits. I would like to express many thanks to Kara Lynch who coordinated the visits very efficiently until August 2017, and to Hanne Heylen who does this as efficiently since then. Thanks also to the many in-house ISOLDE team members from the physics, engineering and operations groups to help guiding several visitors groups per week: last year we had 157 visits, of which 75 groups (external or CERN groups) and 16 VIP groups. The other visits were from professionals or personally organized, mostly one-to-one visits in this case. The visits schedule can be found at this page <http://cern.ch/go/hD8k>.

Becoming the ISOLDE group leader is not an obvious task. Therefore, I want to thank Maria for the two weeks we could spend together in June, where she introduced me at several meetings to many people. I am also extremely grateful to Jenny Weterings and Karl Johnston, who introduced me to all the administrative and technical challenges of ISOLDE and CERN. Finally, it is a pleasure to work with the local team of PhD students and fellows: ISOLDE has at this moment 14 physicists funded through CERN (directly or via our ERC/ENSAR projects): 4 research fellows, 5 applied fellows and 5 PhD students. There are also more than 10 Ph.D. students and post-docs based permanently at ISOLDE, sent from our collaborating institutions. All of them guaranteed a smooth operation of the 46 experiments that ran last year. Also in the target and ion sources groups there are many PhD students and fellows who dedicate their time to provide the ISOLDE users with good beams and who help in developing new beams and ion sources for the future. Together with this enthusiastic team, it is a pleasure to work at ISOLDE.

In 2017, we had a total of 32 weeks or 227 days of protons for ISOLDE. Low energy physics started in April and ran throughout the year until December 4, alternating with post-accelerated beams experiments using the three HIE-ISOLDE cryomodules from July 7 onwards. Of the 27 HIE-ISOLDE experiments that requested beam in 2017, 12 could be scheduled: 9 using the Miniball set-up at XT01, 2 using the scattering chamber at XT03 and 1 using the Edinburgh chamber also at XT03. The ISS magnet was installed at XT02 and its shielding structure was ready in the fall, allowing a successful beam transmission test with the magnet energized just before the end of the running period. The accelerator performed very well last year, with only

1% downtime as compared to nearly 5% in 2016, after some problems with the REX-9-gap amplifier were resolved in the winter shutdown period. This resulted in the double amount of experiments and radioactive beam time delivered by HIE-ISOLDE in 2017, as compared to 2016. Results from the experiments can be found in the contributions to this newsletter, and many were already presented at our ISOLDE Workshop and Users meeting in December (a link to the workshop page can be found here: <http://cern.ch/go/6XpJ>), and which was attended by more than 140 people. Thanks to ENSAR2, users from 44 experiments could be supported for a total of almost 700 days at ISOLDE.

This year's February INTC meeting was the last one where proposals could be submitted to run before the upcoming Long Shutdown 2 (LS2). In the forthcoming meetings, the INTC will review in more detail the physics cases of a few LOIs that were submitted to previous meetings (some of them requesting space in the hall). From November 2018 onwards, the INTC will start reviewing the backlog of experiments and ask for status reports from the different collaborations. The aim is to close experiments which are no longer relevant (on the request of the spokesperson/collaboration or on the request of the INTC) and as such to reduce the backlog significantly by the time we start again in 2021.

I look forward to a successful year of experiments at ISOLDE, before we have to close for 2.5 years. The 4th cryomodule of HIE-ISOLDE has been successfully installed in the tunnel (see pictures on the opening page) and gradual cool down and commissioning of the accelerator has started. All is on schedule to start with accelerated beams for physics on July 9th. In the meantime many low-energy experiments will be performed from April 9th onwards.

Gerda Neyens

## Information for users coming to ISOLDE in 2018

*Karl Johnston, ISOLDE physics coordinator*

### Schedule 2018

ISOLDE will have protons available for physics from April 9<sup>th</sup> till November 12<sup>th</sup>. As in previous years, the schedule for 2018 is split into two distinct periods. While the commissioning of HIE-ISOLDE with four cryomodules takes place, both GPS and HRS will serve low energy physics. This period will run from weeks 15 – 26. HIE-ISOLDE is expected to resume operation from July 9<sup>th</sup>. 2017 demonstrated that interleaving high and low energy runs was an efficient use of ISOLDE and this practice will be maintained in 2018. The ISOLDE schedule can be found at <http://isolde.web.cern.ch/isolde-schedule> and more detailed weekly schedules will be sent around a few days before the beginning of the week concerned.

### User registration for 2018

A full description of the procedure for registering at CERN is given at the end of the newsletter. Visiting teams should use the pre-registration tool (PRT) to register new users. As in 2017, the teamleader and deputy teamleader who sends the information via PRT must have a valid CERN registration. This also applies to paper forms which have been signed at the visiting institute. If the teamleader or deputy do not have a valid registration, the users office will refuse to accept the documents.

### Access to CERN: visible display of ID badges

Starting from May 2nd, it will be required to display visibly CERN badges while on-site. This can be around the neck using the standard CERN lanyard or clipped to an item of clothing. New or replacement lanyards and clips can be obtained from building 55. Full details of the new measures are here: <http://cern.ch/go/Zv9V>.

### Access to ISOLDE: ADAMS

As in 2017 access to ISOLDE is now entirely managed through ADaMS (Access Distribution and Management System). For the uninitiated and experienced user alike, ADaMS can be quite confusing. The access

permission required for ISOLDE is **ISOHALL**. Once submitted it will be sent for approval to the physics coordinator where training ranks will be checked before access is granted.

### Required training courses for access to ISOLDE hall and chemical labs

There are a variety of training courses required before access to the ISOLDE hall can be granted. These are divided into hands-on courses, which take place at the CERN training centre in Preveessin, and online courses which can be taken through the CERN online training.

The courses can be found on two different websites: [cta.cern.ch](http://cta.cern.ch) for hands-on courses and [sir.cern.ch](http://sir.cern.ch) for online courses respectively. Registration should take place via EDH in advance of coming to CERN; in the event that a user is not yet registered an email can be sent to safety training: [safety-training@cern.ch](mailto:safety-training@cern.ch). However, once registered it will be still necessary to register for the hands-on courses in EDH in order to validate the training.

- Pre-requisite online training courses (can be followed prior to arrival at CERN)
  - Safety at CERN (duration: 15 min)
  - Electrical Safety - Awareness (duration 20 min)
  - Radiation Protection - Awareness (duration 10 min)
  - Radiation Protection - Supervised Area (duration 30 min)
- Required hands-on courses
  - ISOLDE - Experimental Hall - Electrical Safety - Handling (course code STELS05IE)
  - ISOLDE - Experimental Hall - Radiation Protection - Handling (course code STIRP06IE)
  - B. 508 chemical labs: The laboratories on the ground floor of 508 where solid state physics perform chemistry also have their own access. It is required to follow the on-line SIR course "Chemical

Safety Awareness” before requesting the permission **ISOICHEM** for 508 R-002 and **ISOEXP** for 508 R-008 for the measurement area.

### Technicians for users at ISOLDE

ISOLDE now has at its disposal the services of two technicians — partly funded from the ISOLDE collaboration — who can assist with mechanical work and installation work for experiments. Their names are Francois Garnier (162968) and Antonio Goncalves Martins De Oliveira (163947). To request any work please contact me.

### Safety in the ISOLDE hall

The wearing of safety helmets and shoes is mandatory inside the ISOLDE hall. It is also mandatory to check yourself on the hand-foot monitor before leaving the ISOHALL zone.

Once within the ISOLDE hall you have at your disposal additional protective equipment such as gloves and contamination monitors to ensure your safety. These are located in the cupboard close to the old control room.

A variety of expert courses are available for those required to perform more demanding operations such as those involving cryogenics, using the crane and lasers. Please ensure that you have followed these courses before performing these tasks.

For those performing electrical work (e.g. making cables, putting up HV cages) a 3-day CERN course needs to be followed (all local physicists have followed it). If you require more information about this, please do not hesitate to contact me.

The mechanical workshop in building 508 is fully operational. If you wish to use it a document will need to be provided which is signed by your team leader, yourself, and our workshop supervisor, authorising you to use the selected machines in the workshop. For more information, please contact your experiment spokesperson, local contact or me.

The list of contacts for safety both for local experiments and visiting setups can be found <http://isolde.web.cern.ch/safety>. All visiting setups

should ensure that they have had a safety inspection before their experiment starts at ISOLDE. Please allow sufficient time for this to be done. You can contact me for more information to prepare for this.

### Publications which have benefited from ENSAR and ENSAR2 funding

Please note that ISOLDE should be mentioned in the abstract of articles related to experiments performed at the facility and, if possible, the ISOLDE team should be mentioned in the acknowledgements. Experiments which have benefited from ENSAR2 funding at ISOLDE should also mention this in the acknowledgements of any articles which emerge and which should resemble the following: *This project has received funding from the European Union's Horizon 2020 research and innovation programme under grant agreement No 654002.*

For experiments which received funding from the first generation of ENSAR funding the following acknowledgement should be included: *This project has received funding from the European Union's 7<sup>th</sup> framework through ENSAR under grant agreement No 262010.*

### Open access policy at CERN

Open access for publications is becoming a requirement for all publicly-funded research. CERN has recently updated its open access policy, which can be found here: <http://library.cern/oa/where-publish>. SCOAP3<sup>1</sup> relates mainly to high energy physics, and adapting this to the output of ISOLDE is not yet completely finalised. At the time of writing the easiest message to pass to the community is the following: papers submitted to the following collection of journals:

- Physical Review Journals (A, B, C, D, E, Lett)
- Nucl Inst and Meth A and B (not proceedings)
- Eur Journal of Physics techniques
- JINST
- Nuclear Physics A and B
- Physics Letters B
- Eur Phys Journal C

which contain at least one CERN author should be

<sup>1</sup>Sponsoring Consortium for Open Access Publishing in Particle Physics

eligible for open access support which can be covered by CERN. However, in order to avoid surprises, it is advised to contact me in advance of submission so that the library can be informed and advise.

### **Publications on CDS**

It is increasingly important that papers from ISOLDE have proper visibility at CERN. To facilitate this, there is a specific area of the CERN Document Server from which all ISOLDE spokespeople and contacts will be able to upload DOI links (and extra information if required). Once you have signed in with your CERN credentials, you should be able to upload any new articles or theses. The link can be found here: <http://cern.ch/go/9lhw>. If there are any problems with uploading, please contact me.

### **Overleaf subscriptions**

CERN is providing free Overleaf Pro+ accounts for all employees, including users, who would like to use a collaborative, online LaTeX editor for their projects.

Overleaf is designed to make the process of writing, editing and producing your research papers and project reports much quicker for both you and your collaborators. Overleaf can also be linked to other services such as Mendeley, Git and Plot.ly to best fit into your workflow.

In order to claim your free 20GB Pro+ account for Overleaf sign into [www.overleaf.com](http://www.overleaf.com) with your CERN email address.

### **ORCID for researchers**

ORCID (Open Researcher and Contributor ID) is a non-profit organization — partly funded by CERN — which is supported by a global community of organizational members, including research organizations, publishers, funders, professional associations, and other stakeholders in the research ecosystem, which has developed a unique researcher identifier that makes it easier to identify your publications. An ORCID account enables you to hold a record of all your research activities, variants of your name, affiliations, etc and is a unique identifier that can accompany you throughout your career, as affiliations, and sometimes also names, change.

CERN is encouraging all users to obtain an ORCID so as to remove any ambiguities which can occur for publications. Registration is relatively easy and generates a unique ID that you can use every time you publish a paper; the link to the ORCID website is here <https://orcid.org/>. If you wish, you can add information about your affiliation and publications. You can also define whether specific data within your record will be private or public.

### **Removal and shipping of equipment from the ISOLDE hall.**

All equipment which has been in the ISOLDE experimental hall requires a control by radiation protection before it can be transported elsewhere or back to home institutes. A new buffer zone has been installed in the ISOLDE hall (close to the SAS and the HIE-ISOLDE tunnel) which implements the CERN-wide TREC system to ensure that all controlled equipment has traceability. This is now incorporated into the EDH flow for all transport requests from the ISOLDE hall.

### **Building 508 and 275: labs, DAQ rooms and kitchen**

On the ground floor of B. 508, within the CERN RP controlled area, the detector laboratory is now up and running. The chemical laboratory is available for occasional chemical operations, once the appropriate access has been followed, as described above.

Upstairs in building 508 the kitchen is now fully installed comprising a fridge, cooker, microwave and dishwasher. In addition, a variety of coffee machines ranging from capsules to moka pots are available. Needless to say, this should be maintained in a good condition and it is the responsibility of experimental spokespeople to ensure that it is kept in a good state.

Users can also avail of the DAQ room to monitor their experiments outside of the controlled zone. The former solid state laboratory is available for installation and testing of equipment prior to installation in the ISOLDE hall. If you are interested in availing of this, please write to me with a detailed request of the infrastructural needs and the time expected.

Please contact me if you have questions concerning access and use of these labs. The local physics

team can also help you with many aspects of ISOLDE experiments, e.g. turbo and pre-pumps, RP sources, chemicals, etc.

### **Visits to ISOLDE**

Visits to ISOLDE are still possible. A typical visit consists of an overview presentation in the visitors area in building 508 and when possible a tour of the ISOLDE facility itself along the pre-arranged visit

path. In the event of a machine intervention or a conflict with physics which happens to be running, the tour of ISOLDE may be cancelled, and one remains in the 508 gallery area.

All visits are coordinated by Hanne Heylen (hanne.heylen@cern.ch) and she should be contacted well in advance with your wishes.

# ISOLDE facility

## Target and Ion Source Development

*Ferran Boix Pamies, Jochen Ballof, Joao Pedro Ramos, David Leimbach, Reinhard Heinke, for the ISOLDE TISD Team and the ISBM working group*

For the ISOLDE and MEDICIS operation in 2017, a total of 36 target and ion source units were assembled, calibrated and tested by our technicians working in the target assembly lab and the OFF-LINE 1 mass separator. To assure quality and to optimize the target and ion source, yields and release are recorded for every unit that is put on-line, typically before handing over to physics. For the 2017 physics at ISOLDE, 25 fresh targets were delivered and irradiated — first results are presented in this issue. The target units characterization and optimization beam time added up to 13.8 days in total [1]<sup>1</sup>.

To match the user's demand in new, more exotic and more intense beams, the target and ion source assembly undergoes constant developments. This is reflected in the fact that 5 of the targets were pure development units that have been exploited on-line or off-line. The progress of Target and Ion Source Development (TISD) is reported bi-annually to the Group of the Upgrade of ISOLDE (GUI). The strong overlap of the source development activities of the target and RILIS teams are coordinated in the ISOLDE Ion Source development and Beam Manipulation (ISBM) working group.

Below we will give an overview of the on-going activities of the target team and the ISBM working group.

### 1. LIEBE: Liquid Eutectic Lead Bismuth Loop Target for EURISOL

Within the aim of increasing the primary beam intensity in the next generation of RIB facilities, a major challenge is the production of targets capable of dissi-

pating the high energy deposited. In this context, the objective of LIEBE is to validate the concept of a high power target able to produce intense secondary beams of short-lived isotopes. The target consists of a loop in which a flow of Lead Bismuth Eutectic (LBE) is established by an electromagnetic pump. After irradiation by protons, the molten liquid flows through a grid creating a shower. The small volume, and bigger surface, of the droplets (0.4 mm diameter, Ref. [2]), enhances the diffusion, and thus increases the yield for short-lived isotopes. The target includes a heat exchanger in order to extract the heat deposited from both the proton beam and the pump. In addition, to ensure the temperature control of the LBE, heating elements and thermocouples are placed all along the loop, Ref. [3].

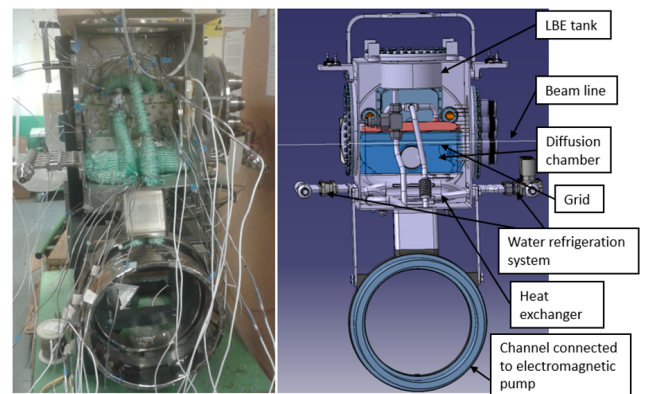


Figure 1: LIEBE target before enclosure, identification of the parts on the 3D model

The prototype is fully assembled and tests were conducted off-line to prove the working conditions of the target. Tests assessing the flow of LBE have shown no cavitation in the range of flow rates necessary for the

<https://isolde.web.cern.ch>

<sup>1</sup>Lower estimate from the tape-station deflector position. Excludes Faraday cup yield estimates and ion source optimizations

droplet formation (0.13 l/s, Ref. [2]), as well as the relation between the pump rotation speed and the developed flow rate. The target was successfully coupled to the OFF-LINE 1 separator and alignment plus vibration tests ensured the stability of the setup target/pump in accordance with international standards for mechanical vibration of rotary parts (ISO10816). However, further off-line tests are now on hold due to the emergence of a vacuum leak when heating up the ion source. It is assumed that thermal dilatation of the vessel containing the ion source reduces the compression of the o-ring seal. Efforts to dissipate the heat and increase the sealing pressure are ongoing to solve the problem.

As soon as the leak is fixed, the tests will continue with the assessment of the heat exchanger dissipated power depending on the LBE temperature, testing of the LIEBE safety systems such as: the LBE level sensors, the LBE leak pressure sensor and the accelerometer evaluating the vibration transmitted by the pump. Finally, the beam contaminants will be evaluated through mass scans of the stable beams produced.

The complexity of the target brings difficulties to its installation in the ISOLDE facility. During the year-end technical stop (YETS), tests with the LIEBE target at ISOLDE were performed and new power cables for the electromagnetic pump were placed to avoid perturbation of the sensors signal. A dedicated room will be prepared as a replica of the ISOLDE target area to rehearse and prepare the final installation of LIEBE planned to go on-line at the end of 2018.

## 2. The upgraded ISOLDE Yield Database

The ISOLDE Yield database is the best source of information about extractable beam intensities and therefore one of the most valuable tools for experiment planning. With the increasing demand for more and more exotic beams, needs arise to extend the functionality of the database and website not only to provide information about yields determined experimentally, but also to predict yields of isotopes which can only be measured with sophisticated setups.

The manual prediction of yields is a time-consuming process in which several parameters have to be con-

sidered. The number of radio nuclides generated inside the target container by the driver beam (in-target production) is the first parameter that has to be addressed by means of costly simulations, which are covered in more detail in the next section. Due to the limited lifetime of radioactive species, a certain fraction of isotopes will already have decayed before completing their journey from the target container to the ion source. This percentage can be obtained by mathematical operations from a release curve of a longer-lived isotope of the chemical element of interest [5]. Currently, release curves for 427 yield entries are available in the yield database.

Release Stable Isotope	
<b>Alpha</b>	0.89
<b>Rise time</b>	0.030 s
<b>Fast fall</b>	0.450 s
<b>Slow fall</b>	7.900 s

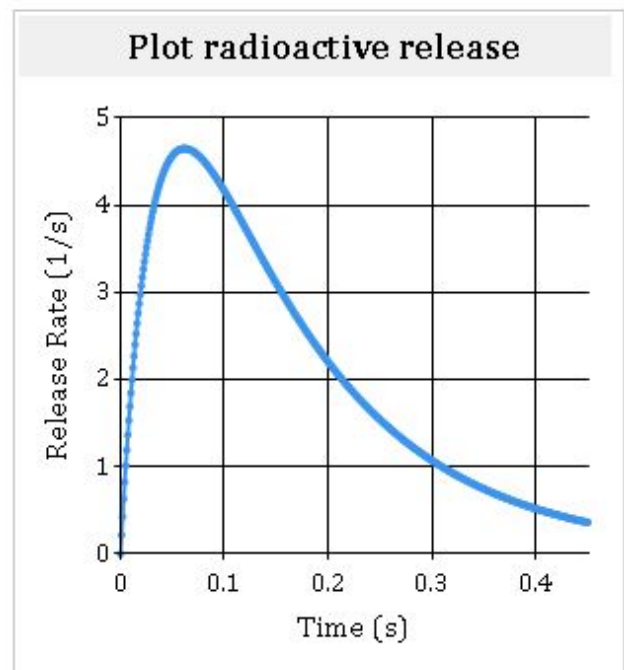


Figure 2: Exemplary release curve information in the yield database. Parameters are discussed e.g. in [4].

Comparing the in-target production multiplied by the release fraction with the measured yield of the same isotope, allows the extraction of a combined parame-

ter that accounts for ionization efficiency, chemical efficiency and other losses.

For cases, in which the release is well understood, the yield database has the capability to store all the necessary data to predict yields in a fully automated manner. Therefore, the website is now being further developed to present this data.

In addition to our efforts in extending the functionality of the yield database application, we were also working on means and processes to introduce yield values more promptly. It is our goal to provide preliminary yield numbers fast but also show evaluated and reliable numbers. Therefore, we introduced a validation status in the yield entry which directly affects the visibility to certain user groups. While users at CERN will have access to non-published yields, the access will be restricted for external users. After undergoing a verification process, the yield status will be promoted and the record made available to the public.

To further improve the yield management, we have equipped our database with a new windows client, allowing faster entry of new datasets and data manipulation. We also contribute to the CRIBE (Chart of Radioactive Beams in Europe) project aiming at the establishment of a common yield database for operational and planned European ISOL-facilities. Therefore, we are implementing a programming interface, which allows the use of yield data in other applications.

You are invited to follow-up the new developments, which are easily accessible through the ISOLDE webpage (<http://cern.ch/isolde>) by following the link to the development yield database, currently shown in the side bar. The legacy yield database is also still available, but is not updated anymore.

### 3. In-Target Production

Yield estimations are provided regularly by the TISD team in order to plan for developments and answer user requests for unmeasured isotopes. With this in mind, a campaign was launched one year ago, to calculate isotope in-target production with high statistics using using ABRABLA [6] and FLUKA [7, 8] codes (the usual codes for yield estimations used at ISOLDE). While

both codes are Monte-Carlo, ABRABLA calculates isotope production cross sections of individual elements while the FLUKA approach is more complex as it calculates particle transport and interaction with matter using several physics models in an input geometry. The codes will be used to simulate isotope production with all the past, current and possible future target materials at proton beam energies of 0.6, 1.0, 1.4 and 2.0 GeV, which sum up to years of cumulated CPU time.

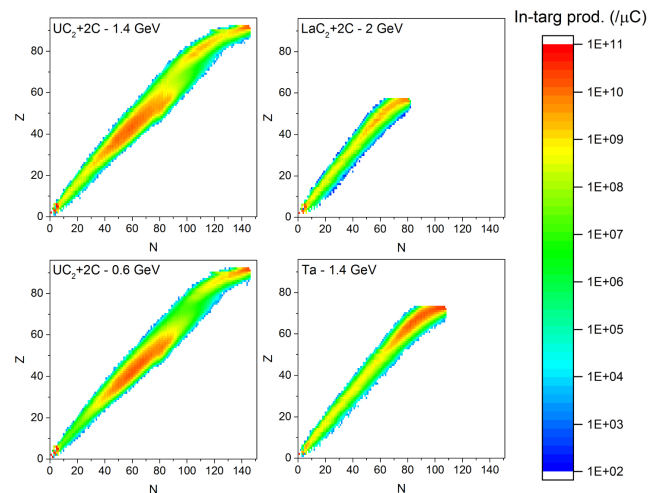


Figure 3: Example of in-target production for  $UC_2+2C$  at 0.6 and 1.4 GeV,  $LaC_2+2C$  for 2 GeV and Ta at 1.4 GeV.

Such systematic simulations can be used to estimate isotope extraction efficiencies from different combinations of targets and ion sources used for the past 50 years at ISOLDE. These estimations can provide a large insight on the release of isotopes from different targets which will be useful for the TISD activities as well as future developments. This data can also be used to calculate yield estimates for specific isotopes that are not yet present in the ISOLDE database, often required by ISOLDE users for proposals. A systematic study of the effect of the ISOLDE 2.0 GeV  $6 \mu A$  driver beam upgrade in the current yields will also be possible, which will provide yield estimates for all targets of high interest for the ISOLDE community.

We plan to make this data available in the yield database where the user will have access to the data in the form of full nuclide charts with cross sections per target material/target element (ABRABLA), in-target production for all current and past ISOLDE target materials (ABRABLA and FLUKA), a tool to customize and

build a target material using ABRABLA cross sections and a yield prediction tool yet to be designed. The simulation parameters as well as ABRABLA and/or FLUKA code version will be made available as well.

#### 4. Negative Ion Source Development

During the negative ion campaign in 2016 the first electron affinity measurement of a radioactive Isotope ( $^{128}\text{I}$ ) was performed as a milestone towards the electron affinity measurement of astatine [9]. In order to facilitate further negative ion studies at ISOLDE, the development program of negative ion beams at ISOLDE was continued in 2017.

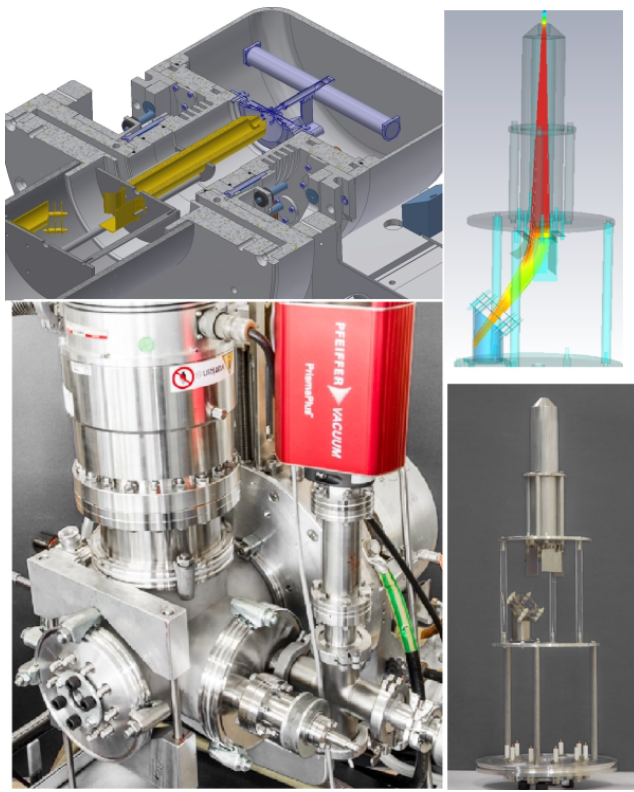


Figure 4: The new ion source test stand. Upper row: 3D CAD model of the test stand (left) and the extraction flange with simulated ion beam (right). Lower row: pictures of the assembled test stand and extraction flange.

To improve long-term testing and general ion source development capabilities, a new dedicated ion source test stand, shown in Fig. 4 was conceived, the two main features being an ion extraction system that allows the measurement of the total ion beam current, and a residual gas analyzer to monitor source degradation and out-gassing.

A data acquisition and control system facilitates the automation of repeated measurement tasks, thereby

also enabling long-term performance tests, rigorous quality control and stress testing. Eventually destructive tests will be performed which will give insight into failure modes and operational limits, the lack of knowledge of which is often a limiting factor in achieving optimal ion source performance under on-line conditions.

In order to improve the ionization efficiency of the negative surface ion source, new low-work function materials were investigated at the new test-stand, promising candidates being  $\text{SrVO}_3$  with a predicted work function of about 1.7 eV [10] and  $\text{GdB}_6$ , previously used in a tubular geometry. As a benchmark of their work function, the thermionic emission of in-house produced  $\text{Sr}_x\text{V}_y\text{O}_z$  and purchased materials such as gadolinium hexaboride  $\text{GdB}_6$  were investigated at the newly built test stand and compared to lanthanum hexaboride ( $\text{LaB}_6$ ), the standard negative ion source material. Initial results showed an electron emission of  $\text{Sr}_3(\text{V}_2\text{O}_4)_2$  comparable to  $\text{LaB}_6$ , with the  $\text{GdB}_6$  electron emission being much lower. The investigation of new negative ion source materials will be continued throughout 2018 in addition to studies of the ionization efficiencies of different source geometries through simulations as well as off-line testing.

#### 5. LIST V2.0: Laser Ion Source and Trap to go on-line

For experiments which demand the highest ion beam purity, the LIST ion source (Laser Ion Source and Trap) was developed in close collaboration between ISOLDE and the University of Mainz. It comprises spatial separation of atomization inside a standard hot cavity, as used by the Resonance Ionization Laser Ion Source (RILIS) [11], and resonant laser ionization in a clean interaction volume. Contaminations arising from surface ionization in the hot environment are suppressed by an electrostatic repelling electrode directly downstream of the cavity, whereas neutral particles can enter an RFQ structure, get element-selectively ionized by the lasers and are guided towards ion beam extraction. This technique was applied on-line to perform hyperfine structure laser spectroscopy on neutron-rich polonium, which was previously inaccessible due to

an overwhelming fraction of easily surface-ionized francium [12, 13].

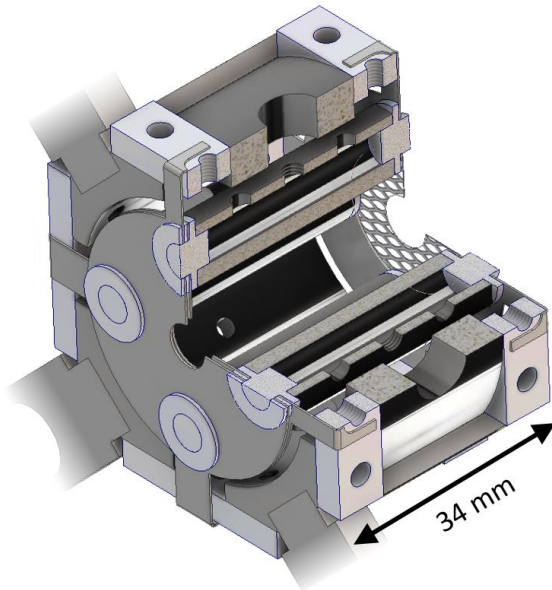


Figure 5: Cut view CAD drawing of the LIST ion source to be used this year. Directly downstream of a standard hot cavity, two repelling electrodes suppress contaminations. Adapted length and a metal mesh at the exit reduce deposition area.

This year, a refined version of the LIST will be used for generation of pure  $^{22}\text{Mg}$  beams to perform measurements on its super-allowed branching ratio and half-life (IS614). The overall geometrical design has been adapted to minimize deposition, while a second repelling electrode ensures additional suppression by inhibiting electron impact ionization inside the RFQ structure, as shown in Fig. 5. At the off-line mass separator, the unit will undergo additional tests to eventually further increase its performance: A DC voltage offset operation mode will shift the produced ions to a different mass regime, sidestepping isobaric contaminations. Using high resistive cavity materials and the LIST as field-free a drift volume will also enable a time-of-

flight based operation mode for short ion bunches and subsequent beam gating purification methods, exploiting the pulsed structure of the RILIS ionization laser system [14, 15].

## References

- [1] J. Ballof, "Isolde workshop and users meeting 2017: **Target operation in 2017**", (2017).
- [2] M. Delonca, 'Development of new target concepts for proton beams at CERN/ISOLDE. Développement d'un nouveau faisceau de protons au CERN/ISOLDE' (2015), PhD Thesis, Presented 14 Dec 2015.
- [3] D. Houngho, *et al.*, *Nucl. Instrum. Meth. B* **376**, 57 (2016).
- [4] M. Turrión, *et al.*, *Nucl. Instrum. Meth. B* **266**, 4674 (2008).
- [5] R. Kirchner, *Nucl. Instrum. Meth. B* **70**, 186 (1992).
- [6] A. Kelic, M. Valentina Ricciardi, K.-H. Schmidt, *ArXiv e-prints* (2009).
- [7] T. Bhlen, *et al.*, *Nuclear Data Sheets* **120**, 211 (2014).
- [8] A. Ferrari, P. R. Sala, A. Fass, J. Ranft, *FLUKA: A multi-particle transport code (program version 2005)*, CERN Yellow Reports: Monographs. CERN, Geneva (2005).
- [9] S. Rothe, *et al.*, *J. Phys. G Nucl. Partic.* **44**(10), 104003 (2017).
- [10] R. M. Jacobs, D. Morgan, J. H. Booske, in *2015 IEEE International Vacuum Electronics Conference (IVEC)*, pp. 1–2 (2015).
- [11] V. Fedosseev, *et al.*, *J. Phys. G* **44**(8), 084006 (2017).
- [12] D. A. Fink, *et al.*, *Phys. Rev. X* **5**, 011018 (2015).
- [13] D. Fink, *et al.*, *Nucl. Instrum. Meth. B* **317**, 417 (2013).
- [14] V. I. Mishin, A. L. Malinovsky, D. V. Mishin, *AIP Conf. Proceedings* **1104**, 207 (2009).
- [15] S. Rothe, *et al.*, *Nucl. Instrum. Meth. B* **376**, 86 (2016).

## RILIS Report for 2017

R & D and operational achievements

*B. Marsh on behalf of the RILIS and ISBM groups*

Here we report on recent operational and development highlights of 2017 for the Resonance Ionization Laser Ion Source (RILIS)[1].

### RILIS hardware consolidation

Several new lasers were installed at RILIS and put into operation for the 2017 physics program:

**Dye pump laser:** A new 100 W, 532 nm EdgeWave Nd:YAG laser was installed to replace the old laser. This new laser has improved beam quality (circular Gaussian beam), resulting in better dye laser performance and improved ease-of-use.

**Ti:Sapphire cavities:** The latest generation of Mainz LARISSA Z-resonator cavities were installed and used at RILIS during 2017. The new lasers, designed by T.Kron (Mainz) feature improvements for easier alignment and simplified switching between operating modes (intra-cavity doubling, dual-etalon narrowlinewidth) [2]. The previous-generation RILIS Ti:Sa cavities have been adapted to include several enhancements taken from the new lasers (alignment points, additional mounting holes) and are now in use at the auxiliary laboratories (OFFLINE 1 and LARIS).

**Laser for non-resonant ionization:** A second Coherent Blaze Nd:YVO<sub>4</sub> laser was ordered at the beginning of 2017. Unfortunately the company has decided not to manufacture this laser so we plan to investigate an alternative solution during 2018.

### RILIS operation

Below is a summary of the RILIS operation, accounting for more than half of the ISOLDE physics in 2017:

- 21 different elements: In, Mg, Mn, Al, Bi, Cd, Sn, Se, Sm, Ni, Dy, Nd, Ga, Li, Hg, Mo, Cu, Sc, Ti, Si, Te.
- 21 separate on-line runs
- 95 days of on-call operation for physics.

### RILIS beam development

In the last year new schemes for Ti, Se, Sm and Sc were tested. A highlight of the RILIS beam devel-

opment was the first measured yield of RILIS-ionized scandium isotopes at ISOLDE, made possible with the use of the ISOLTRAP MRTOF-MS for isotope identification. Figure 1 shows the scandium ionization scheme and measured yields. Secondly we have demonstrated the suitability of single-colour, two-step ionization scheme for samarium. This is extremely convenient since it is a means of producing a RILIS-ionized beam with only one tunable laser. This greatly simplifies the laser setup required for the planned RILIS ion source development activities at the off-line separator that will continue throughout 2018 (new LIST testing, high resistance cavities, VADLIS). The efficiency of the single-colour, two-step Sm scheme will be measured at ISOLDE before on-line operation in 2018.

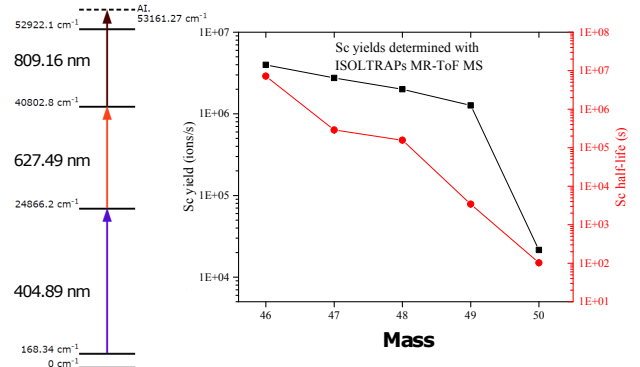


Figure 1: The new combined TiSa and dye scheme for scandium (LHS) and the yields measured using the ISOLTRAP MR-ToF MS (RHS).

### New VADLIS design for improved RILIS-mode efficiency

The Versatile Arc Discharge and Laser Ion Source (VADLIS) has become an established ion source option for ISOLDE users. In 2017 for example, the ability to switch from VADIS-mode to RILIS-mode for liquid-Pb target No.619 to achieve the required purity of <sup>206</sup>Hg for MINIBALL (isobaric Pb contamination was dominant in VADIS-mode) turned out to be crucial for this experiment. The yield measurements indicate an equivalent

RILIS-mode and VADIS-mode ionization efficiency for Hg. To date all on-line applications of the VADIS have used an unchanged VADIS design (the Mk5 FEBIAD anode geometry). As one of the many activities of the Ion Source and Beam Manipulation (ISBM) working group, we have been investigating options to optimize the VADIS for RILIS-mode operation. As a first step, we sought to address the fact that reducing the anode voltage to operate in RILIS-mode results in a corresponding reduction of the ion source extraction voltage. This is because the extraction voltage is provided by the 1.5 mm exit hole of the anode, which is isolated from the anode body and directly connected to the high voltage platform (the extraction potential is therefore equal to the anode voltage). A new VADIS prototype, equipped with an independent voltage-controllable extractor aperture, was built and tested at the ISOLDE offline separator. Figure 2 shows this new VADIS prototype. It offers the additional advantage of increasing the structural stability of the anode itself, corresponding to an inherent reliability improvement of the ion source. This work and the accompanying particle-in-cell simulations of the ion source form part of the PhD thesis of Y. Martinez (KU Leuven)[3]. The offline tests show that at least a two-fold increase in RILIS-mode ioniza-

tion efficiency has been achieved. These results were later confirmed in an on-line test at ISOLDE, with efficiency improvements of a factor of 2-7 measured for RILIS-ionized Mg, Mo and Hg.

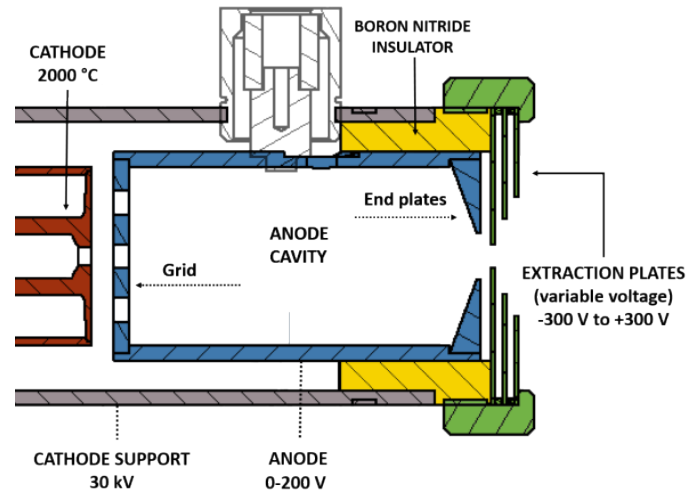


Figure 2: The VADIS prototype with variable extraction voltage

## References

- [1] V. Fedosseev, *J. Phys. G Nucl. Partic.* **44**(084006) (2017).
- [2] T. Kron, *PhD Thesis, University of Mainz, LARISSA Group* (2017).
- [3] Y. Martinez, *in preparation*.

## Summary of the Operations of REX/HIE-ISOLDE during the 2017 Campaign

*Jose Alberto Rodriguez  
for the HIE-ISOLDE project and BE-OP-ISO*

The 2017 high-energy campaign started at the beginning of July right after the beam commissioning of the third cryomodule was completed. The first radioactive beam was delivered on July 7<sup>th</sup>. A  $^{72}\text{SeCO}^+$  beam was produced in the GPS target and transported to the REX-TRAP and REX-EBIS where the molecules broke and the  $^{72}\text{Se}$  was charge-bred. The optimal charge state ( $^{72}\text{Se}^{19+}$ ) was selected in the REX separator and the beam was injected into the linac and accelerated to 4.4 MeV/u before delivering it to the Miniball spectrometer. The Physics campaign continued for 20 more

weeks until Nov. 29<sup>th</sup>. During this time, twelve experiments (Table 1) were conducted. Fifteen different isotopes (as light as  $^9\text{Li}$  and as heavy as  $^{206}\text{Hg}$ ) with energies between 3.4 and 8.0 MeV/u were delivered to three different experimental stations (the Miniball spectrometer at the end of XT01, and the Scattering and Edinburgh chambers at the end of XT03). Stripping foils were used in two of the experiments ( $^9\text{Li}$  and  $^{15}\text{C}$ ) to clean beam contaminants.

In total, 1508 hours of RIBs were delivered to the users during the campaign. In addition, 492 hours of

stable beams were provided to test and calibrate different systems in the experimental stations.

Table 1: Beams provided during the high-energy Physics campaign.

Exp.	Beams	Origin/Destination	E [MeV/u]	Hours
IS628	$^{28}\text{Mg}^{9+}$	HRS / XT01	5.5	176
IS607	$^{59}\text{Cu}^{20+}$	GPS / XT03	3.6 - 5.0	133.5
IS547	$^{206}\text{Hg}^{46+}$	GPS / XT01	4.2	84
IS561	$^9\text{Li}^{3+} \rightarrow ^9\text{Li}^{3+}$	GPS / XT03	8.0	80
IS562	$^{108}\text{Sn}^{26+}$	HRS / XT01	4.5	94
IS546	$^{142}\text{Sm}^{33+}, ^{140}\text{Nd}^{33+}$	GPS / XT01	4.6	166
IS572	$^{94}\text{Rb}^{23+}$	GPS / XT01	6.2	140
IS619	$^{15}\text{C}^{5+} \rightarrow ^{15}\text{C}^{6+}$	GPS / XT03	4.35	245
IS558	$^{140}\text{Sm}^{34+}$	GPS / XT01	4.65	113
IS553	$^{142}\text{Ba}^{33+}, ^{144}\text{Ba}^{33+}$	GPS / XT01	3.4, 4.2	147
IS569	$^{70}\text{Se}^{17+}, ^{66}\text{Ge}^{16+}$	GPS / XT01	4.4	97
IS597	$^{72}\text{Se}^{19+}$	GPS / XT01	4.4	33

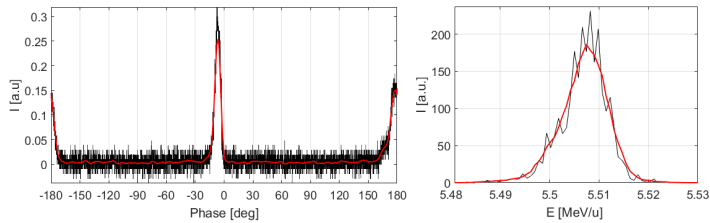


Figure 1: Phase scan completed as part of the phasing procedure of the second SRF cavity of the first cryomodule (on the left). Measurement of the energy and energy spread of the  $^{28}\text{Mg}^{9+}$  beam before it was delivered to the Miniball spectrometer (on the right).

With the exception of the  $^9\text{Li}$  experiment when the gradient of the SRF cavities had to be pushed to the limit, the post-accelerator was very stable. The downtime associated with trips of the REX normal conducting cavities went down from 4.9% in 2016 to 1.3% in 2017. The reliability of the superconducting cavities also improved and the downtime associated to their

trips was reduced from 2.0% in 2016 to 1.1% in 2017. There were only two important interventions that resulted in significant downtime (16 hrs. due to a LHe loss in one of the cryomodules and 6 hrs. due to the failure of a component of an REX RF amplifier). However, there were also several other problems not related to the post-accelerator that had an impact on the experiments. Especially relevant were the lower than expected production yields for the Li and the Se beams and the radiation issue during the Rb run.

Lastly, it is worth mentioning that many improvements related to operations of the linac were introduced in 2017. Particularly important were the new methods to phase the SRF cavities and to measure the energy and energy spread of the beams (Fig. 1). The Fast Beam Investigation (FBI) software (Fig. 2) was also introduced at the end of the year by E. Fadakis and his team. FBI continuously monitored the status of all the devices relevant to the beam delivery and warned the user when one of the devices had an issue. It was used during the last weeks of the year and it helped identify problems with the machine a lot faster than in the past.

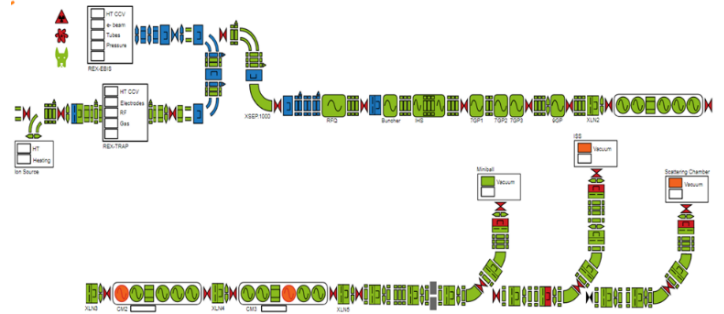


Figure 2: User interface of the Fast Beam Investigation (FBI) of the REX/HIE-ISOLDE post-accelerator.

# Ground-state properties

## High-resolution laser spectroscopy of the neutron-rich tin isotopes

Results of experiment IS573

Liss Vázquez Rodríguez  
for the COLLAPS-ISCOOL collaboration

The IS573 experiment aimed to provide charge radii and electromagnetic moments of ground and isomeric states along the isotopic chain of tin. The program included two independent measurements dedicated to different transitions in the neutral atom. Excitations from the ground state at 286-nm resolved the magnetic moment while the 452-nm transition from a metastable state improved the sensitivity to the quadrupole moment. Both measurements constitute a data set which is being analyzed self consistently in order to obtain the highest possible accuracy for all the parameters.

A major goal of IS573 was to propagate the study of tin beyond the  $N = 82$  shell closure in order to observe a possible shell effect in the charge radii which may or may not be present according to various mean-field calculations. Another primary motivation was the study of the quadrupole moments and isomer shifts associated with the unique-parity  $h_{11/2}$  orbital known to have a simple mass dependence in the cadmium analogues. In addition, from a shell-model perspective, the study of the doubly-magic-plus-one-neutron nucleus  $^{133}\text{Sn}$  is considered important due to the anticipated single-particle nature of its ground state.

Hyperfine spectra were observed for all species up to  $^{134}\text{Sn}$  (see spectrum in Fig. 1) which enables us to tackle the points mentioned above. Furthermore, the electromagnetic moments and charge radii of the long-lived isomers in  $^{113,123,128}\text{Sn}$  have been assessed for the first time. Tin has been the subject of multiple studies throughout the years. With respect to

previous laser spectroscopy experiments [1, 2, 3] we have been able to benefit from a number of improvements. The radioactive beams of tin at ISOLDE have been selectively laser ionized, thus aiding the suppression of contaminants, and subsequently bunched for a 10000-fold background suppression in the fluorescence spectra. Furthermore, our measurements were implemented in a collinear geometry, therefore with the highest possible resolution limited fundamentally by the natural linewidth. Simultaneous analysis of the two transitions, being linked by the common nuclear parameters, allows their extraction with higher precision. The overall accuracy of the quadrupole moments will be improved further due to a dedicated computational study of the electric field gradient in the relevant atomic states.

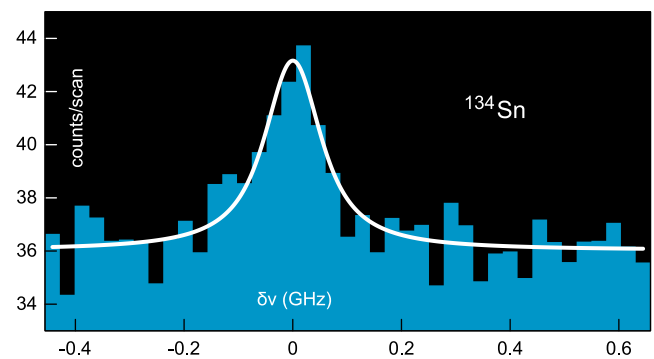


Figure 1: Fluorescence spectrum of  $^{134}\text{Sn}$  in the 286-nm transition in the neutral atom.

## References

- [1] M. Anselment, *et al.*, *Phys. Rev. C* **34**, 1052 (1986).
- [2] J. Eberz, *et al.*, *Z. Phys. A* **326**, 121 (1987).
- [3] F. L. Blanc, *et al.*, *Phys. Rev. C* **72**, 034305 (2005).

## 2017 at the Collinear Resonance Ionization Spectroscopy (CRIS) experiment

Results of experiments IS571, IS620 and IS639

*Cory Binnarsley, Christopher Ricketts and Fredrik Parnefjord Gustafsson for the CRIS collaboration*

During 2017, several successful campaigns were performed at the CRIS experiment. In May, the hyperfine structures of ground and isomeric states of  $^{113-131}\text{In}$  were investigated. From these measurements, the spins, electromagnetic moments, and changes in root-mean-squared charge radii of several states, such as in  $^{131}\text{In}$  (Fig. 1), have been determined for the first time. In June, neutron-rich K isotopes  $^{38-49}\text{K}$  were measured. Despite not reaching our goal of  $^{52-53}\text{K}$ , this experiment provided a rigorous test of our long-term frequency stabilization and demonstrated our ability to achieve the precision required to measure the charge radii of lighter atomic systems. In October, CRIS combined with the TATRA tape station to measure the decay of  $^{80g,m}\text{Ga}$ , providing the laser-ionized selection of ground and isomeric states.

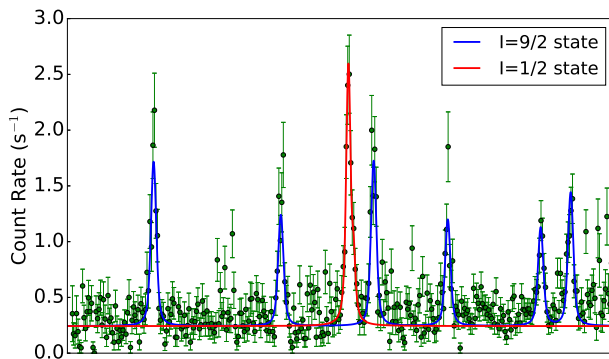


Figure 1: Hyperfine spectrum of  $^{131}\text{In}$ , using the 246.8 nm transition, obtained during IS639. The horizontal axis is frequency (MHz) with a range of 4.5 GHz.

Many of the measurements completed in 2015/16 have now been successfully published, including the ground-state properties of  $^{203}\text{Fr}$ ,  $^{76,77,78}\text{Cu}$ ,  $^{65,67,69,75,79-82}\text{Ga}$  and  $^{222-233}\text{Ra}$  [1][2][3][4]. Furthermore, a paper describing the SATLAS Python package used in the analysis of CRIS data has also been published [5]. Ruben de Groote and Shane Wilkins successfully defended their theses and both graduated

with a PhD. from K. U. Leuven and the University of Manchester, respectively [6].

In preparation for future Sn and In experiments, several stable-beam experiments were performed using the CRIS versatile ion source (CRISIS V) in ablation mode. This provided a pulsed time structure and high-peak ion intensity without the requirement of an RF cooler buncher. This allowed us to assess the efficiency and sensitivity to nuclear observables of numerous laser ionization schemes in both In and Sn, where resolutions down to 50 MHz were achieved. Hyperfine parameters and isotope shifts of several unmeasured atomic states were also extracted.

Several improvements have been made to CRIS throughout the year, such as the recently commissioned event-by-event data acquisition system. This provides a 500 ps time-of-flight resolution, giving us more detailed information on the data acquired. A non-evaporable getter pump was installed in the interaction region decreasing the pressure, by an order of magnitude, to  $1.2 \times 10^{-10}$  mbar. A MagneTOF detector was also installed, increasing the dynamic range and efficiency of our ion detection. These improvements will extend the limits of the experiment's capabilities in the coming year.

## References

- [1] S. G. Wilkins, *et al.*, *Phys. Rev. C* **96**, 034317 (2017).
- [2] R. P. de Groote, *et al.*, *Phys. Rev. C* **96**, 041302 (2017).
- [3] G. J. Farooq-Smith, *et al.*, *Phys. Rev. C* **96**, 044324 (2017).
- [4] K. M. Lynch, *et al.*, *Phys. Rev. C* **97**, 024309 (2018).
- [5] W. Gins, *et al.*, *Comput. Phys. Commun.* **222**, 286 (2018).
- [6] R. P. de Groote, 'CERN-THESIS-2017-154' (2017).

## Collinear laser spectroscopy of nickel

Results of experiment IS568

Simon Kaufmann  
for the COLLAPS - ISCOOL collaboration

Nickel isotopes  $^{58-68,70}\text{Ni}$  were successfully measured in the experiment IS568 using collinear laser spectroscopy (CLS) at the COLLAPS setup in 2016 and 2017. The  $4s\ ^3D_3 \rightarrow 4p\ ^3P_2$  resonance transition in neutral nickel was studied with the goal to shed light on the sub-shell effects around  $N = 40$ . A small distortion of the change in mean square charge radii was observed in neighboring elements [1] and are expected to be stronger for the nickel chain due to the  $Z = 28$  shell closure. The experiment was one of the first to be operated exclusively with the new COLLAPS data acquisition system TILDA. Furthermore, in the second beamtime the stabilization of the Titanium Sapphire laser was considerably improved by using a diode laser stabilized on an atomic transition. The stability of this laser was transferred to the titanium:sapphire laser using a so-called transfer cavity. Finally, the high voltage at ISCOOL, providing the starting potential for the ion beam after cooling, was measured by a precision 50-kV high-voltage divider, on loan from the "Physikalisch-Technische Bundesanstalt" (PTB). Based on these improvements, a better accuracy is expected than that reached in the precursor beamtime in 2016. During the beamtimes, the isotopes  $^{59-68,70}\text{Ni}$  were investigated, crossing the  $N = 40$  sub-shell closure. The investigation of further isotopes was hampered by the slow release of nickel from the target even though the target was operated at very high temperatures beyond usual operation. Efficient ionization of the nickel atoms was realized using resonant laser ionization by the RILIS group. One of the assets of the new DAQ system is that the temporal structure of the bunches from ISCOOL is recorded for each spectrum (see Fig. 1) and can be analyzed on-line and off-line. This provides, for example, information about a possible overfilling of the RFQ,

which immediately becomes visible in a distorted time structure.

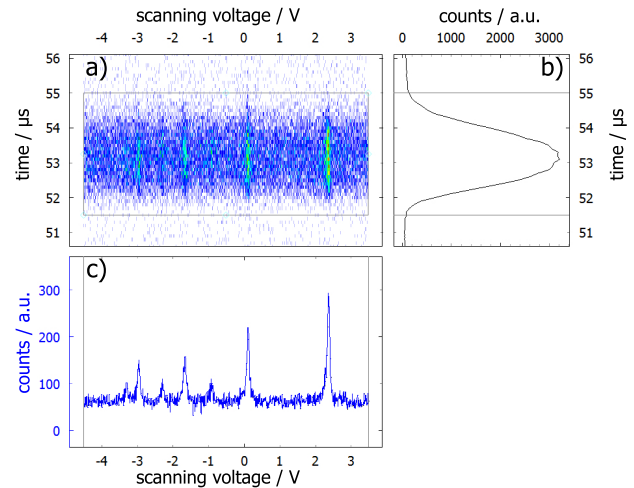


Figure 1: Spectrum of  $^{61}\text{Ni}$  acquired with the new data acquisition system. a) time resolved spectrum: color coded countrate at the photomultiplier tubes as a function of the scanning voltage ( $x$ -axis), which can be converted into a frequency in the rest frame of the ion, and the time of flight of the ions since the extraction from ISCOOL ( $y$ -axis). The grey box is the region of interest (ROI), which is used to constrain the analyzed counts in time and voltage range. b) temporal projection of the number of counts within the ROI onto the time axis, which is expected to be a Gaussian shape in optimized working conditions. c) similar projection onto the voltage axis, which shows the hyperfine structure resonances from which nuclear moments and the charge radii can be extracted.

During the first beamtime this new DAQ ran in parallel to an existing DAQ as a test and after its successful operation it became the main DAQ for the second beamtime. Using field programmable gate arrays (FPGA) as a core of the DAQ the system is highly adaptable for all challenges to come and will serve COLLAPS in the coming years.

## References

- [1] M. L. Bissell, *et al.*, *Phys. Rev. C* **93**, 064318 (2016).

# Precision mass measurements of n-rich cadmium isotopes with ISOLTRAP

Results of experiment IS574

Jonas Karthein for the ISOLTRAP collaboration

The evolution of the  $N = 82$  shell gap for  $Z < 50$  is of great interest for both nuclear structure and astrophysics. The amount by which it is reduced with the removal of protons poses a new challenge to theory and impacts the r-process of nucleosynthesis [1]. This makes it the perfect test case for nuclear models which struggle to describe isotopes far from stability undergoing extreme changes in nuclear structure.

Following beam times in 2014 and 2016, ISOLTRAP continued in 2017 to measure along the cadmium isotopic chain. The isotopes were produced in a uranium-carbide target with neutron converter and quartz insert. For ionization, a RILIS laser scheme was used.

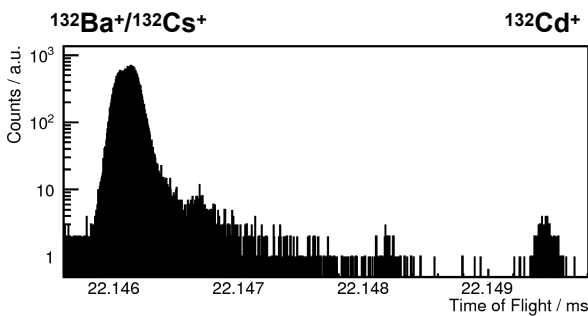


Figure 1: Time-of-flight spectrum obtained with ISOLTRAP's MR-ToF MS showing  $^{132}\text{Cd}^+$  and the isobaric contamination  $^{132}\text{Ba}^+$  and  $^{132}\text{Cs}^+$ .

The yield for  $^{131}\text{Cd}$  was of the order of  $10^3$  ions/ $\mu\text{C}$  and hence sufficient to measure the isotope in the precision Penning trap. The mass obtained confirms ISOLTRAP's published value from 2014 [2] which had been measured by use of the Multi-Reflection Time-of-Flight Mass Spectrometer (MR-ToF MS). The low yield of  $^{132}\text{Cd}$  at that time limited the measurement to the MR-ToF MS. A typical time-of-flight spectrum is shown in Fig. 1. Even though the target was equipped with a quartz inlet, the huge amount of contaminating  $^{132}\text{Cs}$  nuclides saturated the inlet within hours. This left only a short time to measure  $^{132}\text{Cd}$ , however, enough to measure the mass with high precision. It will lead to conclusions about the impact of the nuclide  $^{132}\text{Cd}$  and, via the

two neutron separation energy, about the  $N = 82$  shell strength itself.

The second part of the beam time was dedicated to Phase-Imaging Ion-Cyclotron-Resonance (PI-ICR) [3] measurements of  $^{127}\text{Cd}$  and  $^{129}\text{Cd}$  in the precision Penning trap. This detection technique allowed spatial separation between the ground and low-lying isomeric states of both isotopes. From these measurements their excitation energies could be derived. Figure 2 shows a typical PI-ICR picture for the spatial separation of the ground and isomeric state in  $^{129}\text{Cd}$  for 106 ms phase accumulation time.

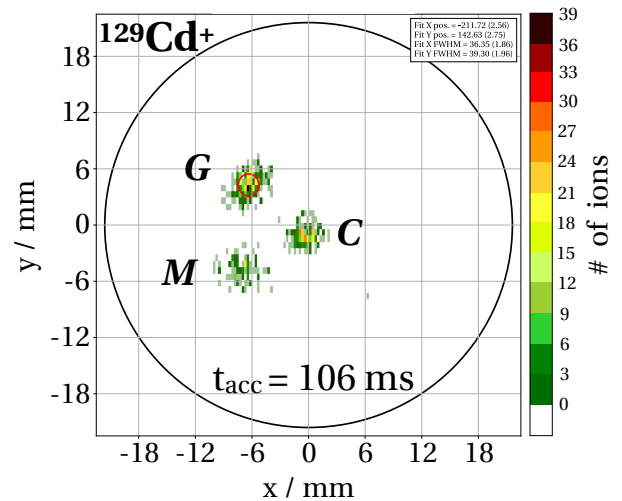


Figure 2: PI-ICR picture of the separation of the ground state  $G$  and the isomeric state  $M$  for  $^{129}\text{Cd}^+$  with the reference spot  $C$  as center of the circular motion.

These results also demonstrate the capabilities of the MR-ToF and PI-ICR techniques at ISOLTRAP, which are currently being further developed.

## References

- [1] M. Mumpower, R. Surman, G. McLaughlin, A. Aprahamian, *Prog. Part. Nucl. Phys.* **86**, 86 (2016).
- [2] D. Atanasov, *et al.*, *Phys. Rev. Lett.* **115**, 232501 (2015).
- [3] S. Eliseev, *et al.*, *Phys. Rev. Lett.* **110**, 082501 (2013).

## ISOLTRAP probes the $N = 28$ shell gap and deformation near $A = 100$

Results of experiment IS490

*M. Mougeot & D. Lunney, for the ISOLTRAP collaboration*

Binding energies from mass measurements give critical clues for nuclear shell closures. Likewise, mid-shell binding energies indicate the effects of deformation. Using the ISOLTRAP mass spectrometer, two such complementary cases were studied last year: the  $N = 28$  shell closure from masses of  $^{46-48}\text{Ar}$  and the phase-transition boundary around  $A = 100$  from masses of  $^{97-98}\text{Kr}$ . These measurements follow previous ISOLTRAP studies of  $^{44-45}\text{Ar}$  [1] and  $^{96-97}\text{Kr}$  [2].

Being noble gases, Ar and Kr ions are readily lost to charge exchange with the neutral buffer gases used in the cooling process necessary for ion trapping. Moreover, Ar and Kr must be ionized with a plasma source, which adds copious contamination to the beams delivered through the mass separator.

As seen from the spectra in Fig. 1, powerful mass separation is required to battle the overwhelming (mostly stable) contamination. This has been accomplished using the ISOLTRAP MR-ToF device [3]. The same spectra were also recorded without protons to confirm the identity of the radioactive species by its disappearance. While the peaks bracketing  $^{48}\text{Ar}$  were not identified,  $^{98}\text{Kr}$  was accompanied by the isobaric  $^{98}\text{Mo}$  and doubly charged  $^{196}\text{Hg}^{2+}$ .

Preliminary results for  $^{46-48}\text{Ar}$  show a relatively strong shell gap for  $N = 28$ . The masses of  $^{97-98}\text{Kr}$  indicate a less pronounced onset of deformation, in contrast with the more sudden shape changes for neighboring nuclides with higher  $Z$ , for example in Rb ( $Z = 37$ ) and Sr ( $Z = 38$ ) also studied by ISOLTRAP [4] and [5], respectively. During the last run, the mass of  $^{97}\text{Kr}$  was also measured with the precision Penning trap. The result compares perfectly with the previous value [2], obtained using the preparation Penning trap with a so-

called cooling resonance using a fit function called Double Woods-Saxon, introduced in [6].

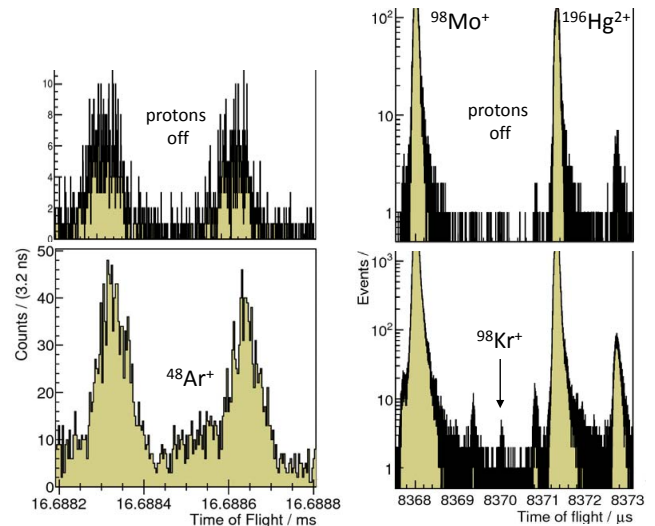


Figure 1: Time-of-flight spectra after the ISOLTRAP MR-ToF-MS recorded for (left)  $^{48}\text{Ar}$  and (right)  $^{98}\text{Kr}$ . The upper panels correspond to the same spectra recorded without protons on the target.

The different components of ISOLTRAP and the recent physics results have been reviewed in the ISOLDE Laboratory Portrait [7].

## References

- [1] K. Blaum, *et al.*, *Phys. Rev. Lett.* **91**, 260801 (2003).
- [2] S. Naimi, *et al.*, *Phys. Rev. Lett.* **105**, 032502 (2010).
- [3] R. Wolf, *et al.*, *Int. J. Mass Spectrom.* **349-350**, 123 (2013), 100 years of Mass Spectrometry.
- [4] V. Manea, *et al.*, *Phys. Rev. C* **88**, 054322 (2013).
- [5] A. de Roubin, *et al.*, *Phys. Rev. C* **96**, 014310 (2017).
- [6] S. Naimi, *et al.*, *Hyperfine Interact.* **199**(1), 231 (2011).
- [7] D. Lunney (on behalf of the ISOLTRAP Collaboration), *J. Phys. G* **44**(6), 064008 (2017).

## New territory for IDS – hyperfine structure and isotope shift measurements

Results of experiment IS608

*J. G. Cubiss, A. N. Andreyev, A. E. Barzakh  
for the Windmill-RILIS-ISOLTRAP-IDS collaboration*

The summer of 2017 saw the first application of the Isolde Decay Station (IDS) for hyperfine structure (hfs) and isotope shift (IS) measurements. The combination of the tape station, silicon detectors and high-efficiency clover type germanium detectors, makes IDS the perfect tool for the performance of hfs and IS measurements, using the  $\alpha$ - $\beta$ - $\gamma$ -decay tagging methods.

Prior to the experimental work, a dedicated effort was made by members of the IDS and Resonance Ionization Laser Ion Source (RILIS) collaborations, in order to create a communications system between the respective setups. This development represents an extension of the successful Windmill-ISOLTRAP-RILIS collaboration, which over the past years has undertaken an extensive campaign of in-source laser spectroscopy studies in the lead region [1, 2, 3, 4]. The addition of the IDS to the collaboration provides more flexibility and sensitivity in otherwise difficult cases, such as the separation of isomers in long-lived beta-decaying isotopes.

During the IS608-2017 run, hfs and IS measurements were successfully performed on 13 ground and isomeric states in the bismuth isotopes  $^{188,193,195,197,200,203,214,215}\text{Bi}$ . Confirmation was made of the large and unexpected staggering/coexistence at  $A = 188$  ( $N = 105$ ) observed during the IS608-2016 run, which appears at the same neutron number as the famous staggering in the mercury isotopes [5]. However, unlike in the  $I = 1/2$  mercury isotopes, the extraction of the quadrupole moments for the  $I > 1/2$  states in bismuth nuclides was possible in our experiment. In addition to this, intruder isomer shifts in the neutron-deficient bismuth isotopes were confirmed by the new data. The results extend the available data for the intruder isomer chain up to  $A = 203$  ( $N = 120$ ), the

closest intruder isomer measurement to the  $N = 126$  shell closure, to date. In the neutron-rich isotopes, thanks to the high  $\gamma$ -ray detection efficiency of IDS, a new high-spin isomer was identified in  $^{214}\text{Bi}$ , for which a dedicated decay study was made. In addition to this, the results for the high-spin isomer  $^{215}\text{Bi}^m$  (see Fig. 1) provide new insight into the shell effect in nuclear charge radii.

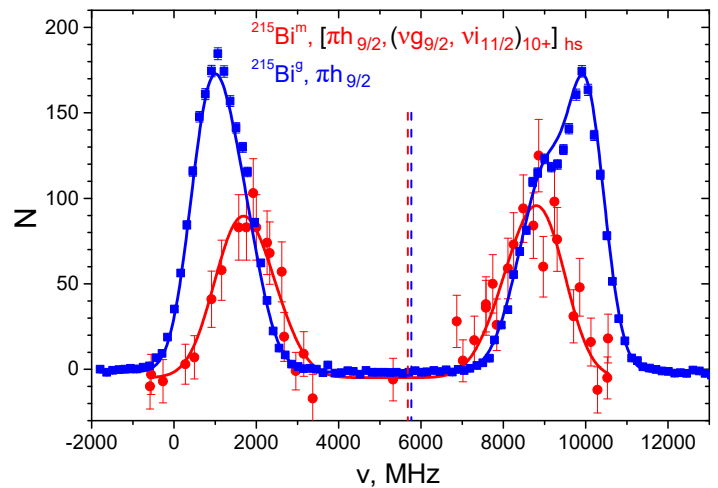


Figure 1: Hyperfine structure spectra for  $^{215}\text{Bi}^g$  (blue squares) and  $^{215}\text{Bi}^m$  (red circles), recorded during the IS608-2017 run. The vertical dashed blue and red lines indicate the centre of gravity for the ground and isomeric state, respectively. Their proximity indicates that the two states have the same mean-squared charge radius.

## References

- [1] H. De Witte, *et al.*, *Phys. Rev. Lett.* **98**(11), 16 (2007).
- [2] T. E. Cocolios, *et al.*, *Phys. Rev. Lett.* **106**(5), 1 (2011).
- [3] A. E. Barzakh, *et al.*, *Phys. Rev. C* **95**(1), 014324 (2017).
- [4] J. G. Cubiss, *et al.*, *submitted for publication* (2018).
- [5] G. Ulm, *et al.*, *Z. Phys. A* **325**(3), 247 (1986).

## Beta-decay studies

### Beta decay of $^{64}\text{Ge}$ for accurate weak-decay rates

Preliminary results of experiment IS570

*E. Náchér for the TAS collaboration*

Nucleosynthesis in explosive hydrogen burning at high temperatures ( $T > 1$  GK) is characterized mainly by the rapid proton capture (rp-) process. Discussions of the possible scenarios for such extreme conditions can be found in [1], where Type I X-ray bursts (XRBs) are suggested as possible sites for the rp-process. In these explosions, temperature ranges between 1 and 3 GK and density between  $10^6$  and  $10^7$  g cm $^{-3}$ . At these extreme conditions beta decay may proceed from excited states and the electron capture process may occur with free electrons from the continuum [2]. Consequently, the weak-decay rates, of paramount importance in astrophysical network calculations, cannot be derived directly from the experimental half-lives in terrestrial conditions, instead theoretical models must be used, and a thorough experimental work is needed to both validate and constrain these models.

In order to constrain the QRPA calculations used in [2] to calculate B(GT) distributions and estimate weak-decay rates near the proton drip line, we carried out an experiment at ISOLDE in May-2016. The goal of our measurement was to apply the Total Absorption Spectroscopy (TAS) technique to the beta decay of  $^{64}\text{Ge}$ , a waiting point nucleus in the  $N = Z$  line. For this purpose we used a production target of ZrO, and separated the isotope of interest in the GeS molecular form. A yield of 200  $^{64}\text{GeS}$  ions per second was measured at the ISOLDE tape station. The separated beam was implanted on tape and moved to the center of LUCRECIA, our large NaI(Tl) crystal, where we measured the gamma-rays after the beta decay of the sample. Ancillary detectors for the detection of beta particles (plastic scintillator) and X rays (planar HPGe detector) completed the setup.

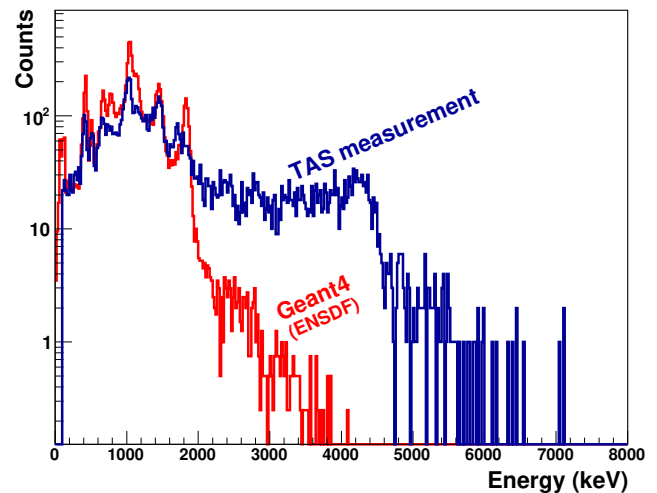


Figure 1: X-ray gated TAS spectrum measured during the IS590 run (blue) compared to the Geant4 simulation (red) of the same decay with the same TAS detector (data from ENSDF). Both histograms contain the same number of counts.

Obtaining a B(GT) distribution from TAS data requires a rather complex analysis, in particular, any statistical method used to unfold the data requires as an input a very clean spectrum and a certain knowledge of the decay scheme. In the process of filtering the data to get a clean spectrum of  $^{64}\text{Ge}$  we have set gates in the X-rays of the daughter  $^{64}\text{Ga}$ , measured with the HPGe planar detector, to tag the electron capture process as well as some fraction of the  $\beta^+$ -decay that populates levels de-exciting via conversion electrons. The gamma spectrum recorded by the TAS under these conditions is the blue line shown in Fig. 1. In the same plot, the red line is a Monte Carlo Geant4 simulation of the same decay under the same conditions. The nuclear data used for the simulation have been taken from ENSDF. We observe that both spectra follow the same pattern up to  $\approx 2$  MeV but there is a large discrepancy from that energy up to the  $Q_{EC}$  value (4.5 MeV). This reflects

the amount of beta population misplaced in the high-resolution measurements so far, and translates into a fraction of B(GT) missing at high energies that is vital for the validation of theoretical models.

## References

- [1] H. Schatz, *et al.*, *Nucl. Phys. A* **777**, 601 (2006).  
 [2] P. Sarriguren, *Phys. Rev. C* **83**, 025801 (2011).

## Electron capture of $^8\text{B}$ into highly excited states of $^8\text{Be}$

Experiment IS633

*Silvia Viñals-Onses for the IS633 collaboration*

The experiment IS633 aims to study the  $2^+$  doublet at 16.6 and 16.9 MeV excitation energy in  $^8\text{Be}$ , which are populated via  $\beta^+$  decay and electron capture (EC) of  $^8\text{B}$ . In addition, we are interested in the so far unobserved EC-delayed proton emission from the 17.6 MeV state. Assuming a factorization of the  $^8\text{B}$  wave function into  $^7\text{Be} + p$ , an upper limit of the branching ratio to this 17.6 MeV state decaying into  $^7\text{Li}+p$  is estimated to be  $2.3 \times 10^{-8}$  [1].

The experiment was divided into two parts. The first was focused on the  $2^+$  doublet. These two states are interesting due to their special configuration, dominantly  $^7\text{Li} + p$  for the 16.6 MeV state ( $\Gamma=108.1(5)\text{keV}$ ) and  $^7\text{Be}+n$  for the 16.9 MeV state ( $\Gamma=74.0(4)\text{keV}$ ) [2]. The feeding of the latter will be an indication of isospin mixing that we would like to evaluate. The second part of the experiment (hopefully scheduled this year) will be dedicated to detecting an experimental limit of the branching ratio of the EC-delayed proton emission from the 17.6 MeV state. The difficulty of this second part is two fold: the extremely low branching ratio and the low energy (337 keV) of the emitted proton.

con telescopes surrounding the C-foil and a 1000  $\mu\text{m}$  DSSSD on the bottom. Two types of telescopes were used: the thicker ones (60  $\mu\text{m}$  DSSSD + 1500  $\mu\text{m}$  PAD) stopped all the  $\alpha$  on the  $\Delta E$  detector. The thinner ones (40  $\mu\text{m}$  DSSSD + 1000  $\mu\text{m}$  PAD) had lower  $\beta$  response. By analysing the  $\alpha$  spectra and taking into account the known decay scheme, we obtain an average yield of  $^8\text{B}$  of  $1.8 \times 10^4$  ions/ $\mu\text{C}$  assuming a transmission to the IDS of 60% .

### Ongoing analysis

Up to now, an accurate energy calibration of the different detectors has been done. Fig. 1 shows the upper part of the energy spectrum corresponding to the sum of the  $2\alpha$  observed in opposite detectors. The observed peaks have centroids compatible with the position of the  $2^+$  doublet. For the highest energy peak assigned to the feeding of the 16.9 MeV state, we estimate about 400 counts. Previously [3] only 5 counts were detected in this zone. The present statistics will allow for precise determination of the branching ratios to these two levels.

### Description of the experiment

The availability of a boron beam at ISOLDE is very recent. The first positive test was done in 2015 with an estimated yield of  $^8\text{B}$  of  $10^4$  ions/ $\mu\text{C}$ . The beam was produced from a target that consisted of pellets of multi walled carbon nanotubes to avoid the aggressive reactions of  $^8\text{B}$  with other materials inside the target. The  $^8\text{BF}_2$  beam (mass 46) was sent to the IDS chamber to be implanted in a carbon foil ( $30 \mu\text{g}/\text{cm}^2$ ). The setup used at IDS consisted of a chamber with 4  $\Delta E$ -E sili-

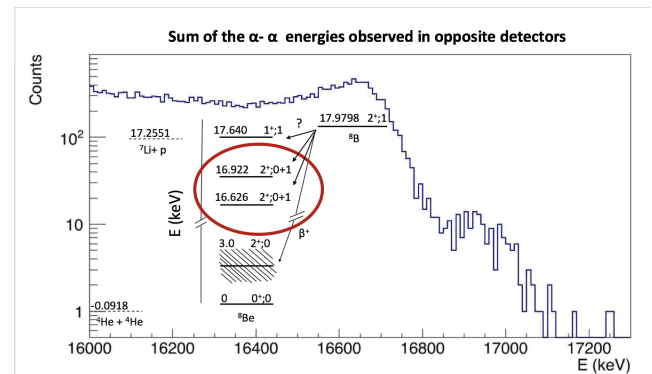


Figure 1: The  $\alpha + \alpha$  energy sum spectrum from  $\alpha$ 's observed in opposite detectors. In the inset we show the  $^8\text{Be}$  decay scheme. The  $\beta$  feeding to the 16.9 MeV state has been observed for first time.

The analysis is still ongoing and the evaluation of this data with R-matrix theory will provide a precise determination of the  $\beta$ -feeding to these states and from that the Gamow-Teller strength and the isospin mixing will be deduced.

## References

- [1] T. N. et al., *Hyperfine Interact.* **129**, 67 (2000).
- [2] *TUNL Nuclear Data Evaluation* (1984).
- [3] O. K. et al., *Phys. Rev. C* **83**, 065802 (2011).

## First $\beta$ -NMR experiments with liquids at VITO

Results of experiment IS645

Stavroula Pallada for the IS645 team

Alkali metal ions play an important role in living organisms and Nuclear Magnetic Resonance (NMR) is one of the most powerful tools to investigate their interaction with proteins, DNA and RNA. However, for most biological systems the direct detection of metal-NMR signals at physiological concentrations in liquids is difficult motivating the idea to use the ultra-sensitive  $\beta$ -NMR technique.

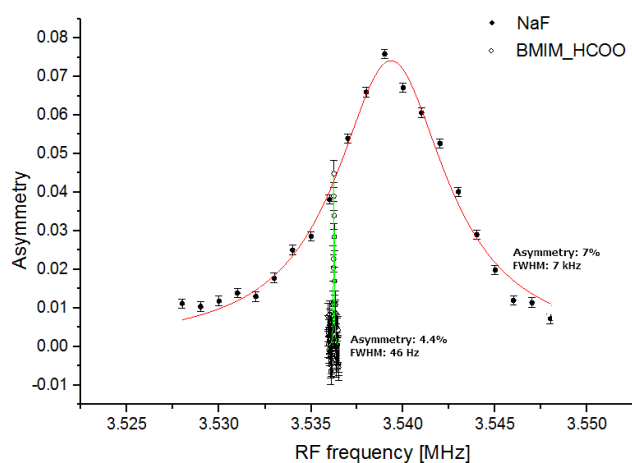


Figure 1:  $^{26}\text{Na}$  resonances of NaF crystal and BMIM\_HCOO ionic liquid.

In 2017, within IS645 two successful  $^{26-28}\text{Na}$   $\beta$ -NMR experiments took place at the recently commissioned laser-polarization setup at VITO [1]. In September we commissioned the new liquid-NMR vacuum chamber, the liquid handling system, the differential-pumping system (providing a vacuum-liquid interface), as well as new compact  $\beta$ -detectors that use Si PMTs. The first NMR spectra at VITO were recorded in a NaF crystal proving that the laser polarisation setup and the RF system were working as envisioned. The first at-

tempt to measure NMR signals from a liquid sample indicated that the magnetic field homogeneity was too low to resolve expected shifts in Na NMR signals in liquids. Thus, before the next beamtime we worked on improvements of the homogeneity of the magnetic field and the liquid handling system was further improved. As a result, in December, the first well resolved NMR signals in liquids were acquired. Among the used ionic liquids, the  $^{26}\text{Na}$  NMR signal in BMIM\_HCOO (1-ethyl-3-methylimidazolium methanoate) showed about 150 ms relaxation time and 10 ppm (parts per million) width. We also attempted to record the first  $\beta$ -NMR spectrum of a short DNA sequence dissolved in BMIM\_HCOO [2]. In Figure 1, the NMR resonance of BMIM\_HCOO is presented in comparison with the NaF resonance.

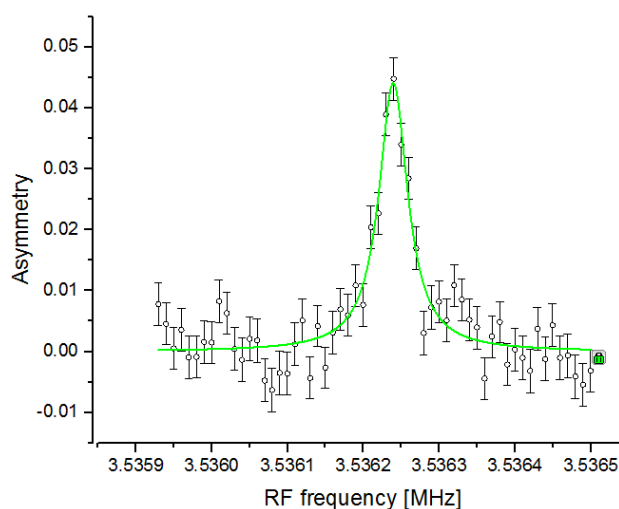


Figure 2:  $^{26}\text{Na}$  resonance of BMIM\_HCOO.

Since December, complementary NMR measurements using stable  $^{23}\text{Na}$  were performed at Poznan University. These are currently undergoing analysis, to

improve the interpretation of the results from ISOLDE. For 2018 our goal is to perform the 1st  $^{26}\text{Na}$   $\beta\text{NMR}$  in truly biological solutions. We aim to study the interaction of Na ions with special DNA-sequences, known as G-quadruplexes [3].

## References

- [1] M. Kowalska, *et al.*, *J. Phys. G Nucl. Partic.* **44**(8), 084005 (2017).
- [2] M. Kowalska, *et al.*, *CERN-INTC-2018-019/INTC-P-521-ADD-1*.
- [3] M. Kowalska, *et al.*, *CERN-INTC-2017-071/INTC-P-521* (2017).

# RIB applications to solid-state physics

## Atomic-scale study of the amorphous-to-crystalline phase transition mechanism in GeTe thin films

Results of experiments IS501 and IS578

Roberto Mantovan and Karl Johnston  
for the eMS collaboration

Chalcogenide materials are chemical compounds containing at least one chalcogen ion i.e. an element from group VI of the periodic table. In particular, the term describes the sulphides, selenides and tellurides.

These materials are characterized by fast and reversible phase transitions, which are typically accompanied by orders of magnitude variations in their electrical resistivity, as well as by large differences in their optical reflectivity, making them extremely important for non-volatile memory applications. Typically, such phase transitions are correlated with electrically/optically-induced fast and reversible switching between amorphous and crystalline phases above room temperature (RT). GeTe is one such material whose study has been recently revived from both fundamental and technological points of view, in different fields ranging from phase-change memories to spintronics [1]. This note presents a summary of recent results in GeTe thin films, which are of interest as a phase change material.

$^{57}\text{Fe}$  emission Mössbauer spectroscopy (eMS) has allowed the study[2] — at the most atomic-scale — of important aspects governing the amorphous-to-crystalline phase transition in GeTe. Following the dilute implantation of  $^{57}\text{Mn}$  ( $T_{1/2} = 1.5\text{min}$ ) decaying to  $^{57}\text{Fe}$ , changes in the electronic charge distribution and local environment occurring around the implanted Fe probe — which substitutes for Ge ( $\text{Fe}_{\text{Ge}}$ ) — across the phase transition were investigated. The unique sensitivity afforded by eMS — especially due to the smaller intrinsic linewidth of the 14.4keV transition — allowed this phase transition to be characterised for the first time. Exper-

imental data were complemented by *ab initio* calculations.

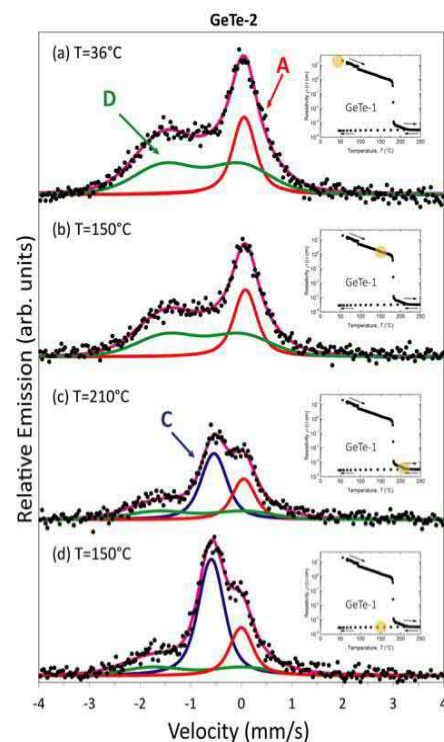


Figure 1:  $^{57}\text{Fe}$  emission Mössbauer spectra obtained on a GeTe thin film held at the temperatures indicated. Insets show the corresponding resistivity state as measured on a separate sample.

Fig. 1 shows sample spectra as the amorphous to crystalline phase transition is traversed. Clear differences either side of the phase transition temperature of  $180^\circ\text{C}$  are seen: the dominant A line cedes to a new component labelled C which represent  $\text{Fe}_{\text{Ge}} - 4\text{Te}_{\text{nn}}$  and  $\text{Fe}_{\text{Ge}} - 6\text{Te}_{\text{nn}}$  respectively i.e. the main effect of the phase transition is the conversion from tetrahedral to defect-free octahedral sites. These results — detailed in [2] — have permitted the mechanism driving

the phase transition to be studied across and during the phase transition for the first time and are a showcase for the power and sensitivity of emission Mössbauer spectroscopy.

## Potassium self-diffusion in single-crystal alkali feldspar

Results of experiment IS492 and IS626

F. Hergemöller for the SSP collaboration

The rock-forming alkali feldspars belong to the most abundant minerals in the Earth's crust and are formed as a solid solution between the sodium ( $\text{NaAlSi}_3\text{O}_8$ , albite) and potassium ( $\text{KAlSi}_3\text{O}_8$ , orthoclase) end-member compositions. Well-founded knowledge of self-diffusion data in alkali feldspar is a prerequisite for interpreting existing *interdiffusion* data [1] that, in turn control re-equilibration features in alkali feldspar that pertain to evolution and dynamics of the crust [2].

We present results from our beam time measuring the  $^{43}\text{K}$  ( $t_{1/2} = 22.3\text{ h}$ ) diffusion in natural gem-quality single-crystal alkali feldspar in the direction normal to (001). After implantation, each sample was annealed at temperatures between 1169 to 1021 K for 20 min to 3.2 h in an integral high vacuum diffusion facility (Online Diffusion Chamber). The samples were then serial-sectioned by ion-beam sputtering with a depth resolution of 24 to 90 nm. Each section was separately collected on a kapton film and transported to a NaI-detector to determine its  $\gamma$ -ray count rate.

The results of four  $^{43}\text{K}$  depth distributions in alkali feldspar after diffusion annealing are presented in Fig. 1 [3] together with results for the as-implanted sample. To prevent overlapping and intersecting data, the measured profiles were individually shifted along the ordinate. It can be seen from the figure that all diffusion lengths are at least ten times larger than the mean implantation depth, i.e.,  $x_0 = 51\text{ nm}$ .

Furthermore, a characteristic decline in tracer concentration towards the surface is observed in all experiments. It seems less likely that this effect is based on a

## References

- [1] R. Bez and A. Pirovano, *Mat. Sci. Semicon. Proc.* **7**(4), 349 (2004).
- [2] R. Mantovan, *et al.*, *Sci. Rep.* **7**(1), 8234 (2017).

supersaturation of vacancies due to implantation damage, since at the high temperatures employed a virtually immediate equilibration is expected. In contrast, it was assumed that the surface acts as an almost perfect sink for the tracer atoms during the diffusion annealing. A suitable solution of the diffusion equation was fitted to the data to derive the corresponding self-diffusion coefficients  $D_K^*$ .

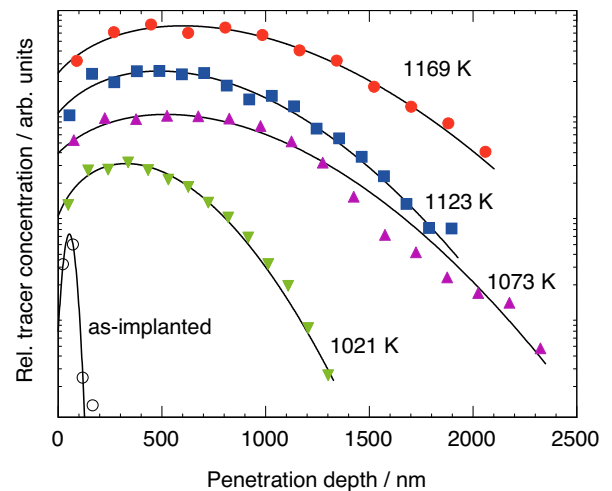


Figure 1: Diffusion profiles of  $^{43}\text{K}$  in alkali feldspar normal to (001) for different annealing temperatures and times. Solid lines represent least square fitting to the data. To enhance visibility of all slopes the relative concentrations are shifted along the ordinate. The  $^{43}\text{K}$  distribution as-implanted is shown for reference (open circles). From [3].

The temperature dependence of K self-diffusion is described by the Arrhenius relation

$$D_K^*(T) = D_0 \exp\left(-\frac{Q}{k_B T}\right), \quad (1)$$

where  $D_0$  is the pre-exponential factor,  $k_B$  is the Boltzmann constant and  $Q$  denotes the activation energy.

According to a least square fit to  $D_K^*$  the activation energy is given by  $Q = (2.4 \pm 0.4)$  eV and the pre-exponential factor by  $\ln D_0/m^2s^{-1} = -12.2 \pm 3.9$ . The results indicate that self-diffusion of K is more than three orders of magnitude slower than self-diffusion of Na in the same feldspar mineral, which was reported earlier.

## References

- [1] E. Petrishcheva, R. Abart, A. Schaeffer, G. Habler, D. Rhede, *Am. J. Sci.* **314**, 1284 (2014).
- [2] R. Abart, E. Petrishcheva, R. Wirth, D. Rhede, *Am. J. Sci.* **309**, 450 (2009).
- [3] F. Hergemöller, *et al.*, *Phys. Chem. Miner.* **44**(5), 345 (2017).

## Copper diffusion in equiatomic CoCrFeNi high-entropy alloy single crystals

Results of experiment IS627

Daniel Gaertner for the SSP collaboration

High entropy alloys (HEAs) are multicomponent alloys, consisting of a large number of elements in equiatomic or nearly equiatomic concentrations [1]. Such alloys tend to form simple solid solutions instead of complex phases or compounds due to their high configurational mixing entropy [2]. Based on interdiffusion measurements, some core effects in HEAs, i.e. high entropy, severe lattice distortion, cocktail effect and sluggish diffusion are found [3]. One goal is to investigate the sluggish diffusion with the help of tracer-diffusion experiments which has already been refuted by tracer experiments in several of our previous studies.

We present results from our 2017 beam time measuring the  $^{64}\text{Cu}$  ( $t_{1/2} = 12.7$  h) diffusion in  $\langle 001 \rangle$  oriented equiatomic CoCrFeNi HEA single crystals. After implantation, each sample was annealed in a temperature range of 973 – 1173 K for 20 min up to 12 h in an integral high vacuum diffusion facility (On-Line Diffusion Chamber). The samples were then sectioned parallel to the surface using ion-beam sputtering with a depth resolution of 88 – 125 nm. The sections were collected separately on a kapton film and transported to a NaI-detector to determine its positron count rate.

The results of three  $^{64}\text{Cu}$  depth distributions in equiatomic CoCrFeNi HEA single crystals after diffusion annealing and the result for the as-implanted sample are presented in Fig. 1. In order to prevent overlapping and intercepting of the measured profiles, the

datasets were individually shifted along the ordinate. Figure 1 shows, that the bulk-diffusion length is between twenty and thirty times larger than the mean implantation depth  $y_0 = 17$  nm.

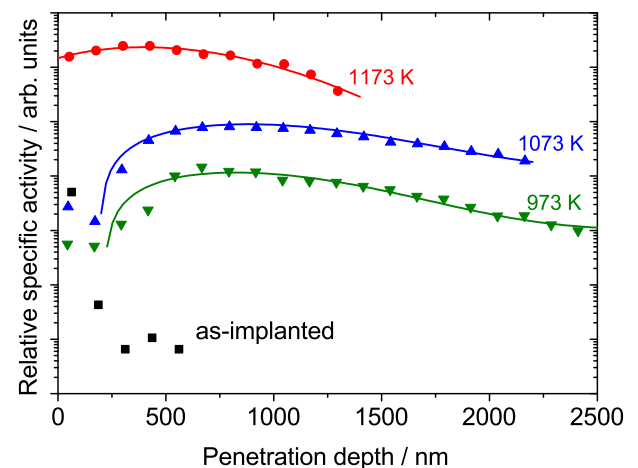


Figure 1: Diffusion profiles of  $^{64}\text{Cu}$  in equiatomic CoCrFeNi HEA single crystals ( $\langle 001 \rangle$  orientation) for different annealing temperatures  $T$ . Least square fitting to the data are represented by solid lines. The relative specific activities are shifted along the ordinate in order to enhance the visibility of all profiles. For reference, the  $^{64}\text{Cu}$  distribution as-implanted is shown (black squares).

Furthermore, in all experiments a characteristic decrease of tracer concentration towards the surface is observed. It was correspondingly assumed that the sample surface acts as an almost perfect sink for the  $^{64}\text{Cu}$  atoms during the diffusion annealing. In order to derive the accompanying bulk-diffusion coefficients  $D_{\text{Cu}}^*$ , a suitable solution of the diffusion equation was

fitted to the penetration profiles.

The temperature dependence of Cu bulk-diffusion in CoCrFeNi is found to follow an Arrhenius behavior

$$D^*(T) = D_0 \exp\left(-\frac{Q}{RT}\right), \quad (1)$$

where  $D_0$  is the pre-exponential factor given by  $D_0 = (6.6_{-5.0}^{+19.5}) \times 10^{-10} \text{ m}^2\text{s}^{-1}$ ,  $R$  is the gas constant and  $Q$  denotes the activation energy given by  $Q = 149.9 \pm 12.1 \text{ kJ/mol}$ , respectively. From the results, one can con-

clude that Cu bulk-diffusion is faster than Co, Cr, Fe and Ni self-diffusion in the same equiatomic HEA at the given temperatures.

## References

- [1] B. Murty, J. Yeh, S. Ranganathan, *Elsevier* (2014).
- [2] J. Yeh, *et al.*, *Adv. Eng. Mater.* **6**(5), 299 (2004).
- [3] K. Tsai, M. Tsai, J. Yeh, *Acta Mater.* **61**(13), 4887 (2013).

## Influence of Fermi-level on the lattice location of $^{27}\text{Mg}$ in GaN

Results of experiment IS634

Ulrich Wahl for the EC-SLI collaboration

During 2017 the emission channeling experiments of IS634 focused on investigating the lattice location of  $^{27}\text{Mg}$  in the technologically relevant wide band gap semiconductor GaN as a detailed function of implantation temperature and implanted fluence in different doping types: undoped GaN, as well as Si-doped  $n$ -type, Mg-doped  $p$ -type, and Mg-doped as grown (pre-doped with  $2 \times 10^{19} \text{ cm}^{-3}$  stable Mg during growth). The amphoteric nature of Mg, i.e. the simultaneous occupation of substitutional Ga and interstitial sites previously reported [1], was fully confirmed ( Fig. 1 ): following ultra-low fluence ( $\sim 2 \times 10^{10} \text{ cm}^{-2}$ ) room temperature (RT) 50 keV implantation, the interstitial fraction of Mg was highest (20-25%) in the two Mg-doped samples and lowest ( $\sim 8\%$ ) in Si-doped  $n$ -GaN, while undoped GaN showed an intermediate interstitial fraction of  $\sim 12\%$ . However, while for implanted fluences up to  $4 \times 10^{12} \text{ cm}^{-2}$  hardly any change at all was observed in the interstitial fraction in undoped and in  $n$ -GaN, in  $p$ -type GaN following implantation of  $1 \times 10^{12} \text{ cm}^{-2}$  of  $^{27}\text{Mg}$  it decreased to the  $\sim 12\%$  level found for undoped GaN; in as-grown Mg-doped GaN, a similar decrease occurred but already at a fluence of  $2.5 \times 10^{11} \text{ cm}^{-2}$ , i.e. around four times faster.

Raising the implantation temperature above RT, the amount of interstitial  $^{27}\text{Mg}$  initially increased in all types of samples, most pronounced in both Mg pre-doped

samples, where interstitial fractions around 30% were reached for ultra-low fluence implantation at  $400^\circ\text{C}$ .

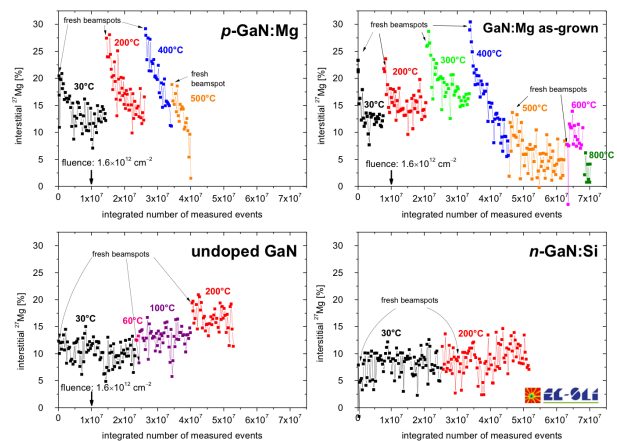


Figure 1: Fractions of interstitial  $^{27}\text{Mg}$  in different doping types of GaN and for various implantation temperatures as a function of the integrated number of events measured (i.e.  $\beta^-$  particles detected) during the experiments. Note that each  $10^7$  events correspond to an implanted fluence of  $1.6 \times 10^{12} \text{ cm}^{-2}$ .

Finally, implanting at temperatures above  $400^\circ\text{C}$  progressively converted interstitial  $^{27}\text{Mg}$  to substitutional Ga sites in all doping types; detailed Arrhenius curves were measured, from which for all four sample types the activation energy for migration of interstitial Mg was estimated to be between 1.3 and 2.0 eV. These results are being interpreted within the framework of Fermi-level dependence of the formation of interstitial vs substitutional Mg. The amount of interstitial Mg formed is highest when the Fermi level is low in the

band gap, i.e. in  $p$ -type material. However, with increasing fluence the implantation-related defects push the Fermi level towards the middle of the band gap, which reduces the amount of interstitial Mg to levels which are similar to undoped material. The fact that this also happens in Mg-predoped samples that were not previously activated indicates that these were actually also  $p$ -type, however, with smaller hole concentration since the effect was faster. The observation that the amount of interstitial Mg initially increases with temperature can be explained by the fact that implantation at elevated temperatures produces less defects so that damage-related shifts of the Fermi level are less

pronounced. Note that an implanted  $^{27}\text{Mg}$  fluence of  $1 \times 10^{12} \text{ cm}^{-2}$  creates an initial vacancy concentration of  $\sim 1 \times 10^{20} \text{ cm}^{-3}$  in the GaN samples, which already exceeds the pre-doped Mg concentration; however, it is not known how many of the implantation defects are electrically active and survive the cool-down of the damage cascade. We also have indications that the amount of interstitial Mg is influenced by changes in the Fermi level due to positive charges building up on the GaN surface during implantation.

## References

[1] U. Wahl, *et al.*, *Phys. Rev. Lett.* **118**, 095501 (2017).

## Results of experiment IS647 in Naturally Layered Perovskites

Results of experiment IS647

*Pedro Rocha-Rodrigues for the IS647 collaboration*

Within the framework of IS647 "Local Probing of Ferroic And Multiferroic Compounds" a comprehensive study on multiferroic materials is ongoing, including materials in which the ferroelectricity order arises from proper, improper and hybrid improper mechanisms. Although the research in the multiferroic field has increased dramatically in the last few years, the number of systems presenting magnetoelectric coupling at room temperature is still very scarce [1]. In this respect hybrid improper ferroelectrics based on naturally layered perovskites (NLP), such as the Ruddlesden-Popper (R.P) phases ( $\text{A}_3\text{B}_2\text{O}_7$ ), have appeared as a fascinating route to design nonexpensive room temperature multiferroic materials [2]. The novel idea behind these NLP is that the ferromagnetic and ferroelectric orders can be coupled through the same  $\text{BO}_6$  octahedral rotation and tilting modes, providing an indirect but very strong magneto-electric coupling [2]. Within the hybrid improper ferroelectrics research field, the IS647 experiment is focused on the R.P.  $\text{Ca}_3\text{Mn}_2\text{O}_7$  and  $\text{Ca}_3\text{Ti}_2\text{O}_7$  phases. In 2011 Benedek and co-workers proposed, by first principles calculations, that both of these compounds should present hybrid improper fer-

roelectricity [2]. Although it has been experimentally observed that near room temperature conditions both of  $\text{Ca}_3\text{Mn}_2\text{O}_7$  and  $\text{Ca}_3\text{Ti}_2\text{O}_7$  present a polar  $\text{A2}_1$ am space group symmetry, until now only  $\text{Ca}_3\text{Ti}_2\text{O}_7$  has presented a switchable ferroelectric polarization [1]. At the moment we are interested in understanding the unique behavior of  $\text{Ca}_3\text{Mn}_2\text{O}_7$ , the structural, charge and magnetic phase transitions that it undergoes and how the multiferroic material properties can be tuned by the partial substitution of Mn by Ti cations. Perturbed Angular Correlation (PAC) measurements were performed successfully at the CERN-ISOLDE facility during  $^{111\text{m}}\text{Cd}$  beam time in 2017. The experimental work targeted specifically the R.P. phase  $\text{Ca}_3(\text{Ti}/\text{Mn})_2\text{O}_7$  series with low Ti doping in the  $\text{Ca}_3\text{Mn}_2\text{O}_7$  parent compound, namely for  $\text{Ca}_3(\text{Mn}_{1-x}\text{Ti}_x)_2\text{O}_7$  and nominal  $x = 0.00, 0.05, 0.10$ . After the radioactive probe  $^{111\text{m}}\text{Cd}$  implantation, the measured samples were submitted to thermal annealing to minimize the crystals lattice defects created by the beam implantation. By comparing PAC time spectrums ( $R(t)$ -function) and its respective Fourier Transform ( $F(\omega)$ ), for different annealing treatments, we found that an annealing in air at  $875 \text{ }^\circ\text{C}$

(and 20 min duration) is suitable for this class of materials. The PAC measurements were performed for several measuring temperatures, in a window range of 11 K to 1153 K. In Fig. 1 well-defined  $R(t)$ -functions for two  $\text{Ca}_3\text{Mn}_2\text{O}_7$  distinct structural and multiferroic phases are displayed. At the moment we are analyzing the acquired data studying the  $\text{Ca}_3\text{Mn}_2\text{O}_7$  types of phase transitions, temperature onsets and the range of co-existence of the distinct phases. The gathered results will enable us to study the  $\text{Ca}_3\text{Mn}_2\text{O}_7$  structural, charge and magnetic phase transitions at the atomic scale, offering us a deeper understanding in this unique system but also guiding us in the development of novel multiferroic materials.

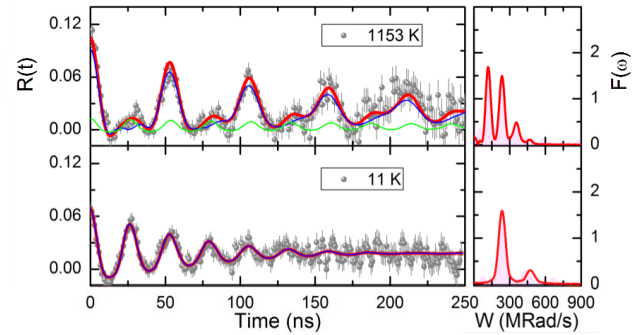


Figure 1:  $R(t)$ -function and  $F(\omega)$  for the  $\text{Ca}_3\text{Mn}_2\text{O}_7$  compound, obtained at: 1153 K, and 11 K.

## References

- [1] B. Gao, *et al.*, *Appl. Phys. Lett.* **110**(22), 0 (2017).
- [2] N. A. Benedek, A. T. Mulder, C. J. Fennie, *J. Solid State Chem.* **195**, 11 (2012).

## Renovation of the emission Mössbauer spectroscopy setup

Mössbauer spectroscopy is a unique technique providing details on electronic, magnetic and structural properties and dynamic processes within materials. Based on recoilless nuclear resonance fluorescence it allows us to probe hyperfine interactions originating from the probe nuclei within their local environment. There are generally three types of hyperfine interactions which originate from the electron density at the nucleus (the electric monopole interaction), the electric field gradient and symmetry (quadrupole interaction) and the magnetic hyperfine field (magnetic dipole interaction). Applying emission Mössbauer spectroscopy (eMS) gives the rare opportunity to study materials with selected short-lived isotopes and at extremely concentrations ( $3 \cdot 10^{12}$  ions  $\text{cm}^{-2}$ ) minimizing implantation-induced damage and changes in the material due to the probe [3].

Mössbauer measurements have been taking place at ISOLDE since the late 1970s; since 1996 the workhorse probe has been  $^{57}\text{Mn}/^{57}\text{Fe}$ . The equipment used for the measurements has constantly been up-

graded since then, although the main base was always maintained. Despite the fact that the setup has been in use for two decades, the slight vibration impact (originating mostly from the forepump) still influences measurements. More crucially, due to the complexity of assembling the setup, a group of people is required to arrive several days prior to measurements. A schematic diagram of the current chamber is shown in Fig. 1.

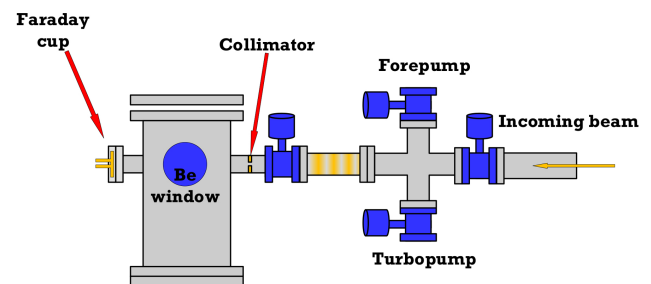


Figure 1: The current experimental setup for eMS experiments.

Furthermore, there are ongoing wet-chemical experiments aiming at getting high oxidation states of implanted  $^{57}\text{Mn}/\text{Fe}$  into various matrices of ferrates. However, due to the current chamber construction, perfor-

mance is limited.

Bearing in mind these aforementioned aspects, the construction of a completely new setup was begun in 2017. This is made from various components such as a pumping system, implantation chamber (see Fig. 2) and electronic module, each mounted on a separated aluminium bed/stand. This allows for shorter preparation times before measurements and eliminates most of the vibrations. Not only does it solve many drawbacks, but measurements can be performed under UV light irradiation with better temperature control.

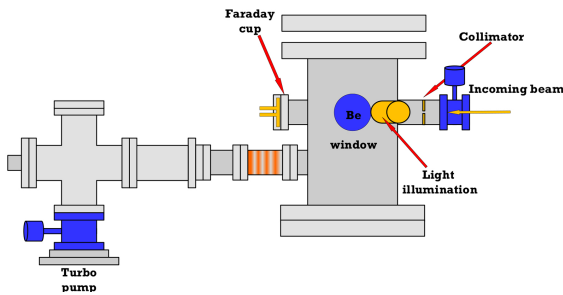


Figure 2: The new eMS setup currently being built. The pumping system is located on the left on a separated CF flange.

Performing measurements under light exposure will allow for insights on the properties of photocatalytic materials, e.g. following changes in the photon field,

acoustic excitations in solids [1]. Hence, this approach can serve as a tool for a profound study of systems such as  $\text{TiO}_2$ ,  $\text{ZnO}$ ,  $\text{CdS}$ ,  $\text{ZnS}$ ,  $\text{GaP}$  and others with various doping.

The current setup has as its major inconvenience protracted pumping times originating from a narrow collimator. To resolve this the pumping system has been updated, vacuum systems are now placed behind the implantation chamber. The new setup is expected to be delivered to the ISOLDE in the middle of this summer. The old setup in its current modification could still be used partially.

The authors acknowledge the financial support by the Federal Ministry of Education and Research of Germany (BMBF), contract # 5K16SI1.

## References

- [1] A. H. Mkrtchyan, *et al.*, *J. Contemp. Phys. (Armenian Academy of Sciences)* **44**(4), 191 (2009).
- [2] G. N. Nadjaryan, *et al.* *Phys. Status Solidi B*, **109**(1), 131 (1982).
- [3] G. Weyer *Hyperfine Interact.* **177**(1) (2007).

# Studies with post-accelerated beams

## Towards Identification of Mixed-Symmetry States in $N=80$ Isotones above $Z=58$

Results of experiment IS546

R. Kern, R. Stegmann, G. Rainovski, N. Pietralla  
for the MINIBALL collaboration

From September 27<sup>th</sup> to October 5<sup>th</sup>, 2017, the first part of experiment IS546 was performed with Coulomb excitation of proton-rich  $^{140}\text{Nd}$  and  $^{142}\text{Sm}$  nuclei at MINIBALL. The aim of the full IS546 experiment is to investigate the restoration of *shell stabilization* [1] when overcoming the  $Z = 58$  subshell closure. First impacts of the crossing of the subshell closure were investigated in experiment IS496, where the  $B(E2; 2_1^+ \rightarrow 0_{1,\text{gs}}^+)$  strength of both aforementioned nuclei were measured [2, 3, 4, 5]. The impact of the  $Z = 58$  proton subshell closure on the isoscalar one-quadrupole-phonon  $B(E2; 2_1^+ \rightarrow 0_{1,\text{gs}}^+)$  strength of  $^{138}\text{Ce}_{80}$  was shown, as well as the restoring of *shell stabilization* above  $Z = 58$ . However, the effect of the  $Z = 58$  subshell closure on the isovector one-quadrupole-phonon valence-shell excitations has not yet been demonstrated. Isovector valence-shell excitations occur in  $N = 80$  isotones between  $Z = 50$  and  $Z = 58$  (sub)shell closures as isolated  $2^+$  states, with nearly no mixing. The isovector  $2^+$  state of  $^{138}\text{Ce}$  ( $Z=58$ ), in contrast, exhibits mixing with other near-lying  $2^+$  states, resulting in a considerable fragmentation of the  $B(M1; 2_{\text{ms}}^+ \rightarrow 2_1^+)$  strength among two or more excited  $2^+$  levels. It is not obvious whether the  $B(M1; 2_{\text{ms}}^+ \rightarrow 2_1^+)$  strength of  $^{140}\text{Nd}$  and  $^{142}\text{Sm}$  is concentrated in a single level or fragmented among several levels. In order to determine the absolute M1 strength, Coulomb excitation yields and multipole-mixing ratios need to be measured. While in the case of Nd the mixing ratios are already known, no information for those in  $^{142}\text{Sm}$  is available.

In experiment IS546 the RILIS ion source was used, with ionization schemes already developed and successfully employed during both parts of experiment

IS496. A tantalum primary target was used to produce RIBs of the desired isotopes, which were post-accelerated by HIE-ISOLDE to 4.6 MeV/u and delivered on a  $^{208}\text{Pb}$  target in MINIBALL for yield measurements.

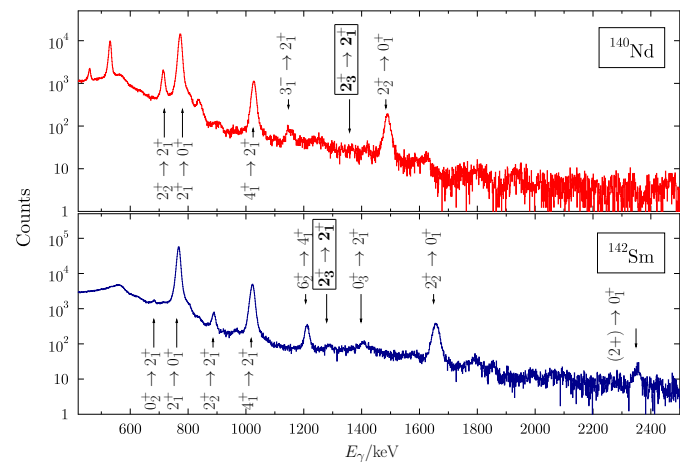


Figure 1: Doppler-corrected, background subtracted and particle gated gamma spectra for  $^{140}\text{Nd}$  and  $^{142}\text{Sm}$ . All identified transitions for both mentioned nuclei are labelled.

Preliminary spectra extracted from the experimental data are shown in Fig. 1 for  $A = 140$  and  $A = 142$ . For the case of  $^{142}\text{Sm}$  the level of statistics is sufficient for determination of the Coulomb excitation yield of the state of interest. The level of statistics for  $^{140}\text{Nd}$  only allows for an identification of the dominant fragment of the  $2_{1,\text{ms}}^+$  state. Therefore, in the case of  $^{140}\text{Nd}$  ( $Z=60$ ), more data are needed for deciding on the amount of fragmentation of the isovector valence-shell mode in a quantitative way. Additional two days of data taking are foreseen in 2018 for a completion of the experiment.

## References

- [1] G. Rainovski, *et al.*, *Phys. Rev. Lett.* **96**, 122501 (2006).

[2] C. Bauer, Ph.D. thesis, Technische Universität Darmstadt (2013).

[3] C. Bauer, *et al.*, *Phys. Rev. C* **88**, 021302 (2013).

[4] R. Stegmann, *et al.*, *Phys. Rev. C* **91**, 054326 (2015).

[5] R. Stegmann, Ph.D. thesis, Technische Universität Darmstadt (2017).

## Coulomb Excitation of Semi-Magic $^{206}\text{Hg}$

Results of experiment IS547

*L. Morrison, K. Hadyńska-Klęk, Zs. Podolyák  
for the MINIBALL collaboration*

Singly and doubly-magic nuclei are of great interest in nuclear physics as they are particularly stable, and as such are spherical in shape. Deviations from this stable core configuration results in nuclear deformation, the nature of which is determined by a number of factors intrinsic to the arrangement of nucleons. One of the most interesting and yet weakly known doubly-magic regions is in the vicinity of  $^{208}\text{Pb}$ .

$^{206}\text{Hg}$  is a singly-magic ( $Z=80$ ,  $N=126$ ) two-proton-hole nucleus with a complex energy level scheme, much of which is unexplored. In particular, just the energy of the  $2_1^+$  state is known while the rest of the low spin level scheme has been only predicted in shell model calculations [1].

In November 2017, a dedicated Coulomb excitation experiment was conducted at the HIE-ISOLDE facility, with  $^{206}\text{Hg}$  being produced using an up to  $0.63\mu\text{A}$  proton beam impinging on a molten lead target, in order to shed light on the unknown structure of this nucleus below the  $10^+$  and  $5^-$  isomeric states, currently inaccessible using other experimental techniques.

$^{206}\text{Hg}$  is, to date, the heaviest radioactive ion beam produced at HIE-ISOLDE. The beam intensity achieved in this experiment was up to  $7.75 \times 10^5$  pps with an energy of 4.19 MeV/u. In order to enhance beam purity by eliminating the stable  $^{206}\text{Pb}$  isobar, laser ionisation was implemented using the RILIS technique. Upon production, ionisation and acceleration, the beam of  $^{206}\text{Hg}$  was Coulomb-excited using two separate targets:  $^{104}\text{Pd}$  and  $^{94}\text{Mo}$ , 2 mg/cm<sup>2</sup> thick each. In this experiment, a DSSSD was placed in the forward direction between 20 and 55° in the laboratory system in order to detect recoiling projectile - and target -like particles, and was

coupled to 24 HPGe detectors forming 8 clusters of the MINIBALL array to detect  $\gamma$  rays. In addition, a thick silicon PAD detector was placed behind the DSSSD detector to collect conversion electrons.

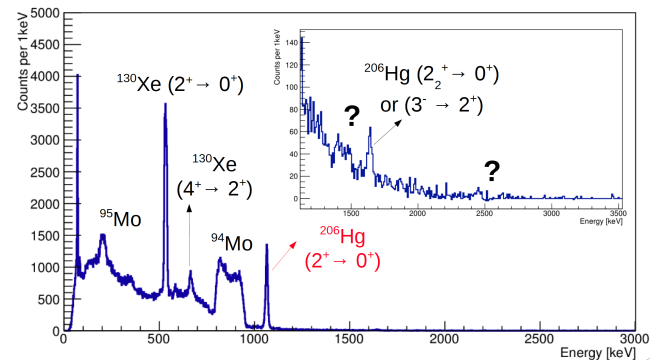


Figure 1: Online  $^{206}\text{Hg}$  beam on  $^{94}\text{Mo}$  target spectrum, Doppler-corrected for the projectile velocity. The  $2^+ \rightarrow 0^+$  transition at 1069 keV in  $^{206}\text{Hg}$  is marked, as well as the excitation of states in stable  $^{130}\text{Xe}$  beam contaminant and the target material.

Prior to the experiment, the GOSIA code [2] simulations of the excitation cross sections were performed in order to predict which transitions could be identifiable during the experiment. The available transition probabilities were taken from the recent SM calculations. It was predicted that the depopulation of the  $2_1^+$ ,  $4_1^+$ ,  $3_1^-$  and  $2_3^+$  states should be visible. The obtained online spectrum collected with  $^{94}\text{Mo}$  target, Doppler-corrected for the velocity of the excited  $^{206}\text{Hg}$  (Fig. 1) has confirmed that we could indeed observe the expected strong  $2^+ \rightarrow 0^+$  transition in  $^{206}\text{Hg}$ , as well as the lines from  $^{130}\text{Xe}$  beam contaminant and other still unidentified peaks which may be contributed to newly observed states in  $^{206}\text{Hg}$ .

The analysis of the experiment is currently ongoing and will allow extraction of transition probabilities in  $^{206}\text{Hg}$ , which in consequence will provide an indication

of the collectivity and deformation in this nucleus.

## References

[1] Z. Podolyák, 'Coulomb excitation of the two proton-hole nucleus  $^{206}\text{Hg}$ ', Proposal to the

ISOLDE and Neutron Time-of-Flight Committee, 29/09/2012, <http://cds.cern.ch/record/1482137/files/INTC-P-340.pdf>.

[2] D. C. T. Czosnyka, C. Wu **28**(745), 1982, [www.slacj.uw.edu.pl/gosia](http://www.slacj.uw.edu.pl/gosia).

## The $^{59}\text{Cu}(p, \alpha)$ cross section and its implications for nucleosynthesis in core collapse supernovae

Results of experiment IS607

*C. Lederer-Woods<sup>1</sup> for the IS607 collaboration*

The origin of the heavy elements (heavier than iron) is one of the most important unanswered questions in modern physics. About 99% of heavy element abundances are produced by neutron capture reactions in the so-called slow and rapid neutron capture processes. About 35 proton rich heavy nuclei, however, cannot be produced by neutron capture reactions. These p-nuclei may be produced explosively by a series of photo-disintegration reactions on pre-existing seed distributions of neutron-rich isotopes (known as the p-process). Models currently fail to reproduce the required high abundances of certain light mass p-nuclei by orders of magnitude [1]. An alternative mechanism is the  $\nu p$ -process that may occur in core collapse supernovae, where intense neutrino winds can create proton-rich ejecta with free neutrons, allowing the formation of proton-rich nuclei [2]. The efficiency of the p-process to produce these nuclei depends on the strength of the  $^{59}\text{Cu}(p, \alpha)$  reaction which may block the process by recycling material back to  $^{56}\text{Ni}$ , creating a closed NiCu cycle [3]. Despite the importance of this reaction for nucleosynthesis, no experimental data are available at present.

In experiment IS607 we have measured the cross section of the  $^{59}\text{Cu}(p, \alpha)$  reaction. This was made possible using a purpose-built detection system provided by the University of Edinburgh and by taking advantage of the high intensity radioactive  $^{59}\text{Cu}$  beam available at HIE-ISOLDE. The  $^{59}\text{Cu}$  beam was impinged on a  $\text{CH}_2$

foil, with  $^4\text{He}$  and  $^{56}\text{Ni}$  particles emitted in the reaction detected in coincidence using two sets of annular silicon strip detectors of type Micron S2.  $^4\text{He}$  ions were detected using a  $\Delta E$ -E telescope placed at a distance of  $\approx 4$  cm to the target, while the  $^{56}\text{Ni}$  recoils that are emitted at much smaller angles were detected with a detector placed at a distance of 40 cm from the  $\text{CH}_2$  target. A photograph of the setup is shown in Fig. 1 The reaction was successfully measured at 5 different beam energies, between 3.6 and 5 MeV/u. The data are currently being analysed.

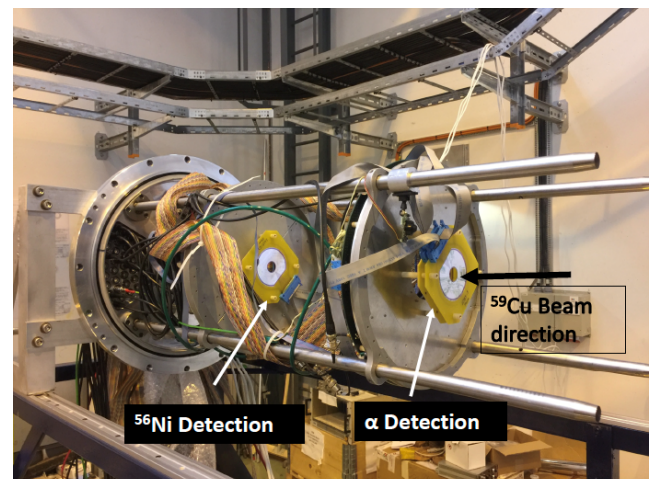


Figure 1: Photograph of the open reaction chamber, showing the detection setup used in this measurement. The  $\text{CH}_2$  target foil was placed about 4 cm downstream of detection setup.

We would like to thank K. Johnston, O. Tengblad, and the Accelerator and RILIS teams for their continuous support in preparation and during the measure-

<sup>1</sup>University of Edinburgh

ment. This work was supported by the Science and Technology Facilities Council UK (ST/L005824/1 and ST/M006085/1), and the European Research Council ERC-2015-STG Nr. 677497.

## References

- [1] M. Arnuold, S. Goriely, *Phys. Rep.* **384**(1), 1 (2003).
- [2] C. Fröhlich, *et al.*, *Phys. Rev. Lett.* **96**, 142502 (2006).
- [3] A. Arcones, C. Fröhlich, G. Martinez-Pinedo, *Astrophys. J.* **750**(1), 18 (2012).

## Magnetic moments of short-lived excited states

Results of experiment IS628

*G. Georgiev and A.E. Stuchbery for the IS628 collaboration*

Magnetic moments of first  $2^+$  states in even-even nuclei are especially sensitive probes of the interplay between their single-particle and collective properties. Usually they do not bear the strong fingerprint of single-particle features, e.g. as the magnetic moments of odd-mass ground- or isomeric states, but rather result from a fine balance between core-excitations and shell-model features.

The aim of experiment IS628, performed in November 2017, was to address the shell-model evolution towards the Island of Inversion around  $^{32}\text{Mg}$ . New calculations by Otsuka *et al.* [1] suggest that sd-pf admixtures may impact the structure of excited states already at  $^{28}\text{Mg}$  and influence its  $g$  factor. For this purpose we applied the Time-Dependent Recoil In Vacuum (TDRIV) technique on H-like charge states [2], for the first time on radioactive ions, to investigate  $g(2^+, ^{28}\text{Mg})$ . Another important milestone for IS628 was the first use of the recently built Miniball plunger device.

The advantage of applying the TDRIV technique on H-like charge states is that the hyperfine field at the nuclear site can be calculated from first principles and no advance knowledge or calibration measurements of the magnetic field is needed. Therefore this technique could provide high accuracy ( $\approx 2\%$ ) magnetic moment values for picosecond-lifetime states.

A test run was performed, using a 5 MeV/u  $^{22}\text{Ne}$  beam from EBIS rest-gas, before starting the experiment with the  $^{28}\text{Mg}$  beam. This allowed us to confirm that the entire setup and the data-acquisition performed

as expected. The results for the ratio function of  $^{22}\text{Ne}$  are presented in Fig. 1 showing the modification of the angular distribution of gamma-rays as a function of the target-degrader distance. This test run was an important ingredient for the follow-up radioactive beam study since it allowed to define with a high precision the absolute target-degrader distance for the plunger device and in this way would reduce the number of parameters for the fit of the  $^{28}\text{Mg}$  ratio function. In addition, the  $^{22}\text{Ne}$  run could provide an important physics result given that the adopted value for  $g(2^+, ^{22}\text{Ne}) = 0.325(10)$  differs by 5 standard deviations from the USD shell model value of  $g = 0.38$ .

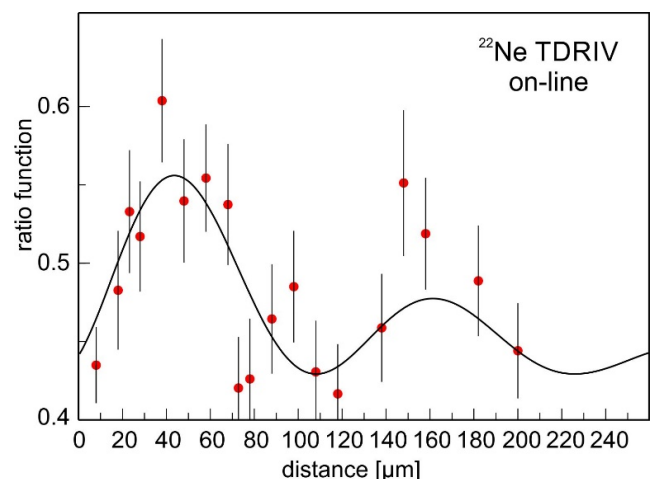


Figure 1: Online results for the ratio function of  $^{22}\text{Ne}$ .

A SiC ISOLDE target was used for the production of  $^{28}\text{Mg}$ . The species of interest were ionized using RILIS and mass separated through the HRS separator before being sent for charge breeding to EBIS and post-accelerated to 5 MeV/u with HIE-ISOLDE Linac.

Excellent beam intensities of few  $10^6$  pps for  $^{28}\text{Mg}$  were available at the Miniball target. However, it appeared that, even with a relatively thin target ( $3.9 \text{ mg/cm}^2 \text{ Nb} + 1.1 \text{ mg/cm}^2 \text{ Ta}$ ) and 29 mm CD-to-plunger distance, the beam scattering inside the Miniball chamber was too high (count rate higher than 10k per Ge crystal per second) which did not allow the use of the full available beam intensity.

The observed gamma-ray angular distribution for  $^{28}\text{Mg}$  was in agreement with the calculated one. The results from the on-line analysis are close to the sim-

ulated pattern and we expect a firm  $g$ -factor result will follow from a careful analysis of the whole data set.

The experiment is to be a part of the PhD thesis of Amar Boukhari (CSNSM, Orsay, France).

## References

- [1] T. Otsuka, INPC 2016 presentation, "Shell Evolution, Shape Transition And Shape Coexistence With Realistic Nuclear Forces".
- [2] A. Kusoglu, *et al.*, *Phys. Rev. Lett.* **114**, 062501 (2015).

## ISOLDE Solenoidal Spectrometer Progress Update

*Robert Page for the ISS collaboration*

Regular visitors to the ISOLDE Hall over the last 12 months will have noticed significant changes as the development of the ISOLDE Solenoidal Spectrometer (ISS) has progressed. Since the recommissioned ISS magnet was moved into the ISOLDE Hall in March 2017, it has been mounted on its support frame, surveyed into position and connected up to the second HIE-ISOLDE beam line XT02. Completion of the magnetic shielding design, fabrication and assembly (see Fig. 1) paved the way for mapping the magnetic field by ISS collaboration members in November 2017, supported by CERN experts.

In the final days before the winter shutdown, a stable beam from HIE-ISOLDE was successfully tuned through the ISS magnet and its profile was monitored as the magnetic field was ramped up. Preparations are now well under way for further stable beam tests, as well as the first experiments with radioactive ion beams later this year. Recent progress includes completing the manufacture of components for the mechanisms for supporting and moving the ISS detector array and targets inside the magnet. These are currently being assembled and commissioned. The first experiments will utilise the Si detector array currently used in the HE-

LIOS spectrometer at Argonne.



Figure 1: Photograph showing the ISS magnet inside its magnetic shielding.

As part of a major UK project a new Si array is being constructed for installation during CERN's second long shutdown (LS2), ready for full physics exploitation thereafter. The supply of the double-sided silicon strip detectors (DSSDs) for this upgrade is also on track, with sufficient DSSDs now having been delivered and accepted to allow completion of the full array (see Fig. 2). The assembly and testing of the detector modules will commence shortly.



Figure 2: Photographs showing an ISS DSSD. In total 24 DSSDs with ASIC readout are required for the full ISS array.

Work is also progressing well on the Leuven-led active target SpecMAT that will be used in separate experiments inside the ISS magnet. A physics workshop to discuss ideas for exploiting the ISS and related spectrometers was held in July. The workshop programme and presentations are available on the ISS collaboration web site (see below). Anyone interested in performing experiments with the ISS is invited to get in touch with the collaboration.

The ISS collaboration acknowledges the strong support for this project at ISOLDE and elsewhere at CERN.

## A new plunger device for MINIBALL at HIE-ISOLDE

*Christoph Fransen<sup>1</sup>, Thomas Braunroth<sup>1</sup>, Alfred Dewald<sup>1</sup>, Liam Gaffney<sup>2</sup>, Alina Goldkuhle<sup>1</sup>, Jan Jolie<sup>1</sup>, Claus Müller-Gatermann<sup>1</sup>, Stefan Thiel<sup>1</sup>, Nigel Warr<sup>1</sup>;*

*<sup>1</sup>Institut für Kernphysik, Univ. of Cologne, Germany, <sup>2</sup>CERN*

The recoil distance Doppler-shift method (RDDS) is a very valuable technique for measuring lifetimes of excited nuclear states in the picosecond range from which absolute transition strengths between nuclear excitations can be deduced. For a number of years this method was intensively used in combination with radioactive beams for investigating exotic nuclei. A new dedicated plunger device including a target chamber was thus built by our group to implement this method at HIE-ISOLDE using multiple step Coulomb excitation or incomplete and complete fusion reactions in inverse kinematics with radioactive beams. Doppler-shifted  $\gamma$ -rays are detected with the MINIBALL spectrometer. The availability of the new plunger device opens excellent prospects for detailed investigations of exotic nuclei at HIE-ISOLDE.

Conditions fulfilled by the new plunger device:

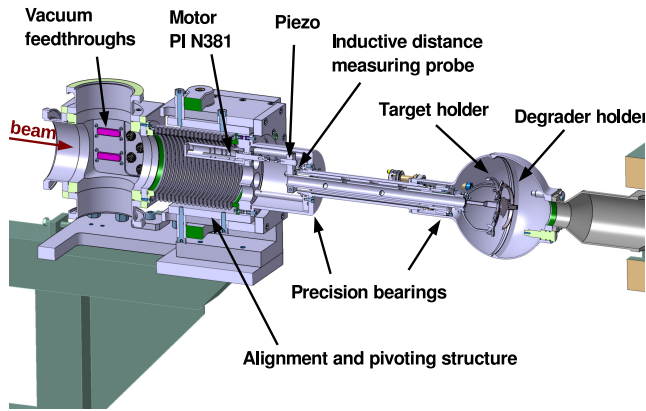
- It is easy to mount and align it at the existing beamline XT01 to allow for a fast and efficient change between different experimental setups.
- It allows MINIBALL detectors to be placed under

angles between 35 and 145 degrees with respect to the beam axis for both lifetime and g-factor measurements. Material within the target chamber was minimized to reduce absorption of  $\gamma$ -rays.

- A high mechanical precision of the distance between target and degrader of  $0.1 \mu\text{m}$  is essential. Therefore, the plunger device also includes a feedback system to guarantee a fixed distance between target and degrader where the latter ranges from contact up to about 15 mm.
- A highly segmented Si detector is placed directly downstream from the plunger target/degrader foils to observe recoils.
- Inside the new chamber the plunger target and degrader holders can be easily replaced with a “standard” target holder.

Figure 1 depicts a lateral cut drawing of the plunger device including the motor (model N381 from Physik Instrumente) to change the distance between target and degrader, the piezo crystal needed for the feedback system and the structure for aligning the plunger and

precisely and reproducibly pivoting it out of the beam-line and back to allow for a safe mounting and aligning of target and degrader.



The plunger device including its computer control was successfully installed at the MINIBALL spectrometer at beamline XT01 in April 2017. A first experiment with the plunger was performed in November 2017 to measure g-factors in  $^{28}\text{Mg}$  (IS 628, spokesperson G. Georgiev). The plunger chamber was used for standard Coulomb-excitation experiments starting from July 2017. In all experiments the new plunger device proved its high capability for ongoing and future experimental campaigns at the MINIBALL spectrometer.

Supported by the German Ministry for Science and Education (BMBF), Grant No. 05P15PKFNA.

Figure 1: Drawing of the new MINIBALL plunger device.

# Support and contacts

## Support and contacts: how to gain access to the ISOLDE hall

---

1. Use the online pre-registration tool<sup>1</sup> which should be launched by your team leader or deputy team leader. You need to attach the following documents to the pre-registration:
    - **Home Institution Declaration<sup>2</sup> signed by your institute's administration (HR).**
    - Passport
  2. When your pre-registration is accepted by the CERN users office you will receive an email telling you how to activate your CERN computer account. Please note however, that your EDH account will not be activated until you arrive at CERN and complete your registration.
  3. When you arrive at CERN go to the Users office to complete your registration (Opening hours: 08:30 — 12:30 and 14:00 – 16:00 but closed Wednesday mornings).
  4. Get your CERN access card in **Building 55**
  5. Follow the online CERN safety introduction course:
    - If you have activated your CERN account, you can access the Safety Awareness course on-line at the web page <http://sir.cern.ch>, from your computer, inside or outside CERN.
    - If you have not activated your CERN account, there are some computers available for use without the need to log in on the first floor of building 55 (Your CERN badge will be needed in order to prove your identity).
  6. Complete the following online courses via <https://sir.cern.ch/sir>:
    - Safety at CERN
    - ISOLDE RP course for Supervised Radiation Areas "Radiation Protection - Supervised Area".
    - Radiation Protection - Awareness.
    - Electrical Safety - Awareness Course.
- If you have not activated your CERN account see the second part of entry 5.
7. Obtain a Permanent radiation dosimeter at the Dosimetry service, located in Building 55<sup>3</sup> (Opening hours: Mon. to Fri. 08:30 12:00). *If you do not need the dosimeter in the following month it should be returned to the Dosimetry service at the end of your visit.* The "certificate attesting the suitability to work in CERN's radiation areas"<sup>4</sup> signed by your institute will be required.
  8. Follow the practical RP safety course and Electrical Awareness Module for which you will have to register in advance<sup>5</sup>. These take place on Tuesday afternoons from 13:00 until 17:00 at the training centre (building 6959) in Preveessin. If you do not have your own transport, you can take CERN

<sup>1</sup>For information see [the CERN users' office](#)

<sup>2</sup>The Home Institution Declaration should not be signed by the person nominated as your team leader.

<sup>3</sup><http://cern.ch/service-rp-dosimetry> (open only in the mornings 08:30 — 12:00).

<sup>4</sup>The certificate can be found via <http://isolde.web.cern.ch/get-access-isolde-facility>

<sup>5</sup>For information about how to register see <http://isolde.web.cern.ch/get-access-isolde-facility>

shuttle 2 from building 500. The timetable for this is [here](#).

9. Apply for access to ISOHALL using ADAMS: <https://www.cern.ch/adams>. This can be done by any member of your collaboration (typically the contact person) having an EDH account<sup>6</sup>. Access to the hall is from the Jura side via your dosimeter. Find more details about CERN User registration see the [Users Office website](#). For the latest updates on how to access the ISOLDE Hall see the [ISOLDE website](#).

New users are also requested to visit the ISOLDE User Support office while at CERN. Opening hours: Monday to Friday 08:30-12:30

#### **ISOLDE User Support**

Jenny Weterings  
 Jennifer.Weterings@cern.ch  
 +41 22 767 5828

#### **Chair of the ISCC**

Bertram Blank  
 blank@cenbg.in2p3.fr  
 +33 5 57 12 08 51

#### **Chair of the INTC**

Karsten Riisager  
 kvr@phys.au.dk  
 +45 87 15 56 24

#### **ISOLDE Physics Section Leader**

Gerda Neyens  
 gerda.neyens@cern.ch  
 +41 22 767 5825

#### **ISOLDE Physics Coordinator**

Karl Johnston  
 Karl.Johnston@cern.ch  
 +41 22 767 3809

#### **ISOLDE Technical Coordinator**

Richard Catherall  
 Richard.Catherall@cern.ch  
 +41 22 767 1741

#### **HIE-ISOLDE Project Leader**

Yacine Kadi  
 Yacine.Kadi@cern.ch  
 +41 22 767 9569

More contact information is available at <http://isolde.web.cern.ch/contacts/isolde-contacts> and at <http://isolde.web.cern.ch/contacts/people>.

<sup>6</sup>Eventually you can contact Jenny or the Physics coordinator.